Pakistan Veterinary Journal

ISSN: 0253-8318 (PRINT), 2074-7764 (ONLINE)
DOI: 10.29261/pakvetj/2025.215

RESEARCH ARTICLE

Evaluating the Antidiabetic, Anticancer, Anti-Alzheimer, Antiviral, and Antimicrobial Activities of Silymarin from Milk Thistle Extract: Hepatoprotective Properties, Histology and Gene Regulators in $HgCl_2$-Challenged Rats

Asmaa Ali Alharbi*[1], Nervana B. Ibraheem[2], Said S. Soliman[2], Tarik A. Ismail[2], Amera N. Alqahtani[3], Jawza A. Almutairi[4], Kamlah Ali Majrashi[5], Amani Osman Shakak[5,6], Aminah Allohibi[5], Eman A. Beyari[7], Hawazen K. Al-Gheffari[7], Maha A. Aljumaa[8], Ahmed Ezzat Ahmed[9,10], Mohsen A. Khormi[11] and Abdallah A. Hassanin[2]

[1]Department of Biochemistry, Faculty of Science, King Abdulaziz University, P.O. Box: 80200, Jeddah 21589, Saudi Arabia; [2]Genetics Department, Faculty of Agriculture, Zagazig University, Zagazig, 44511, Egypt; [3]Department of Biological Sciences, College of Science, University of Jeddah, Jeddah, Saudi Arabia; [4]Department of Pharmaceutical Sciences, College of Pharmacy, Princess Nourah bint Abdulrahman University, P.O. Box 84428, Riyadh, 11671, Saudi Arabia; [5]Biological Sciences Department, College of Science & Arts, King Abdulaziz University, Rabigh, 21911, Saudi Arabia; [6]Faculty of Medical Laboratory Sciences, University of Shendi, Shendi P.O. Box 142, Sudan; [7]Department of Biological Sciences, Faculty of Science, King Abdulaziz University, Jeddah, Saudi Arabia; [8]Department of Biology, College of Science, Princess Nourah bint Abdulrahman University, P.O. Box 84428, Riyadh 11671, Saudi Arabia; [9]Department of Biology, College of Science, King Khalid University, Abha 61413, Saudi Arabia ; [10]Prince Sultan Bin Abdelaziz for Environmental Research and Natural Resources Sustainability Center, King Khalid University, Abha, 61421, Saudi Arabia; [11]Department of Biology, College of Science, Jazan University, P.O. Box. 114, Jazan 45142, Saudi Arabia
*Corresponding author: aanalharbi@kau.edu.sa (Asmaa Ali Alharbi)

ARTICLE HISTORY (25-238)

Received: March 22, 2025
Revised: July 04, 2025
Accepted: July 18, 2025
Published online: August 11, 2025

Key words:
Anticancer
Antimicrobial
Antiviral
Antioxidant
Callus Induction
HPLC
in vitro culture
Phenolic components
in vivo
Liver
Inflammation

ABSTRACT

This study investigated the effects of methyl jasmonate (MeJA) and yeast extract (YE) as elicitors on silymarin yield in cell suspension cultures of *Silybum marianum* L. The main objective was to evaluate the hepatoprotective and gene-regulatory effects of a silymarin-enriched extract (SME), known for its antidiabetic, anticancer, anti-Alzheimer, and antimicrobial properties, in rats challenged with $HgCl_2$. MeJA-treated cultures produced the highest silymarin content, reaching 0.17 mg per 100 g dry weight after 48 hours. High-resolution HPLC analysis revealed that silymarin components in MeJA cultures totaled 595 µg/g, with silibinin A and B accounting for 0.134 mg/g and isosilibinin A and B for 0.025 mg/g of SME. The MeJA-silymarin-enriched extract inhibited α-amylase and glucosidase activities, indicating notable antidiabetic activity. It also demonstrated considerable antimicrobial effects against a range of pathogens, including *Salmonella* Typhi, *Escherichia coli*, *Bacillus cereus*, *Klebsiella pneumoniae*, *Candida albicans*, *Aspergillus niger*, *Fusarium oxysporum*, *Fusarium solani*, *Alternaria alternata*, *Pythium aphanidermatum*, and *Botrytis cinerea*. Antiviral assays showed dose-dependent inhibition of Human parvovirus B19 (PVB-19) and Sapporo virus (SaV) replication *in vitro*, with 89% and 76% inhibition at 100 µg/mL and IC_{50} values of 32 µg/mL and 45 µg/mL, respectively. Moreover, a concentration of 18 µg/mL, SME significantly reduced the viability of 50% of HepG2 liver cancer cells. Furthermore, SME exhibited potent antioxidant activity, reaching 96% DPPH inhibition, and demonstrated distinct neuroprotective effects. For *in vivo* evaluation, 120 Wistar rats were randomly divided into four groups (10 rats per group, in triplicate): a basal diet group, an $HgCl_2$-challenged group, a group fed a diet supplemented with SME (500 mg/kg), and an $HgCl_2$-challenged group treated with SME (500 mg/kg). The SME-treated groups showed significant reductions in the gene expression of precancerous markers (BAX and Casp-3) and proinflammatory cytokines (IL-1β and TNF-α) in $HgCl_2$-stressed rats. These groups also exhibited lower ALT, AST, and glucose levels (a 30% decrease compared to the challenged group), maintained normal liver and intestinal structure, and showed a predominance of beneficial gut microbes compared to the control. Additionally, SME inhibited 86% of acetylcholinesterase (AChE) activity compared to donepezil, supporting its neuroprotective role in $HgCl_2$-treated rats. Collectively, these findings suggest that

MeJA is an effective elicitor for enhancing silymarin production in SME, which may serve as a potent liver protector and gut regulator against oxidative stress.

To Cite This Article: Alharbi AA, Ibraheem NB, Soliman SS, Ismail TA, Alqahtani AN, Almutairi JA, Majrashi KA, Shakak AO, Allohibi A, Beyari EA, Al-Gheffari HK, Aljumaa MA, Ahmed AE, Khormi MA, and Hassanin AA, 2025. Evaluating the antidiabetic, anticancer, anti-alzheimer, antiviral, and antimicrobial activities of silymarin from milk thistle extract: hepatoprotective properties, histology and gene regulators in $Hgcl_2$-challenged rats. Pak Vet J. http://dx.doi.org/10.29261/pakvetj/2025.215

INTRODUCTION

Silybum marianum L., commonly referred to as milk thistle, is a flowering plant in the *Asteraceae* family that serves as a medicinal herb. It is well known for its high content of pharmaceutical-grade antioxidant compounds, including phenolics that exhibit anticancer properties (Shah *et al.,* 2020). Milk thistle contains isomeric flavonolignans collectively known as Silymarin (Albassam *et al.,* 2017), which includes compounds like silydianin, silychristin, silybin, and iso-silybin (IS). Herman *et al.* (2011) demonstrated that silymarin offers significant protection against various oxidants, particularly at the protein level, which directly links it to its use as a hepatoprotective agent for severe liver inflammation, diseases, and fibrosis. Additionally, silymarin possesses antioxidant properties and stimulates protein synthesis and cell regeneration, which may potentially reduce the incidence of certain types of cancer. It can help maintain the structural integrity of liver and kidney cells against the harmful effects of pharmaceuticals, including chemotherapy and radiation, as shown by Saeed *et al.* (2017) and Ghodousi *et al.* (2023). Furthermore, silymarin may prevent neurodegeneration in specific brain regions due to restricted blood flow, with results suggesting that its neuroprotective effects stem from its antioxidant and antitumor properties (Raza *et al.,* 2011).

Plants produce a wide array of bioactive compounds, typically characterized by a predominant class of phytochemicals responsible for their principal health-promoting effects (El-Saadony *et al.,* 2023a,b; Alharbi *et al.,* 2024). These natural bioactive compounds have exhibited potential biomedical applications (Mueed *et al.,* 2023; El-Saadony *et al.,* 2024a; Reda *et al.,* 2024a). Recent research studies have shown that *Silybum marianum*, particularly its active compound silymarin, has demonstrated promising antibacterial and antifungal activities (Alshehri *et al.,* 2022). Additionally, it exhibits antiviral activity against several viruses, including dengue virus and COVID-19 (Low *et al.,* 2021; Zhang *et al*., 2023). This suggests that it may have potential as a natural remedy for various infections (El-Sapagh *et al.,* 2023). Moreover, it showed promising potential in the fight against Alzheimer's disease (AD). Its primary active compound, silymarin, exhibits several properties that may contribute to its neuroprotective effects (Elsawy *et al.,* 2021). However, further research is required to fully elucidate its mechanisms of action and to assess its safety and effectiveness in humans.

Inconsistent and limited production of secondary metabolites in *S. marianum*, influenced by seasonal changes, geographical locations, and environmental conditions, presents a significant challenge (Mosihuzzaman, 2012). *Silybum marianum* exhibits notable variability in secondary metabolite content due to genetic, physiological, ecological, and environmental factors when grown in open fields, resulting in variations in the quality and quantity of its commercial products. Given the substantial commercial demand for *S. marianum*, ongoing efforts focus on refining the cultivation practices of this medicinal herb (Isah *et al.,* 2018).

To overcome these hurdles and ensure the standardized production of biologically active compounds, *in vitro* cultivation of *S. marianum* presents a promising strategy (Graf *et al.,* 2007; Bekheet, 2011). In addition to media modifications, various strategies, including environmental adjustments, the application of elicitors, and the use of precursor compounds or biotransformation techniques, can enhance secondary metabolite production (Ruiz-García and Gómez-Plaza, 2013).

Elicitation is a powerful approach for activating plant defense responses and is considered one of the most effective strategies for enhancing secondary metabolite production in plant cell cultures (Baenas *et al.,* 2014). Elicitors act as triggers, mimicking the effects of naturally occurring plant chemicals and initiating the formation of ROS (reactive oxygen species). These ROS bursts serve as a secondary messenger, enhancing both enzymatic and non-enzymatic defense mechanisms, thereby mitigating the adverse effects of ROS (Abdul Malik *et al.,* 2020). By applying biological or non-biological elicitors, researchers can achieve higher concentrations and productivity of metabolites in shorter periods within in vitro cultures (Smetanska, 2008). Nevertheless, identifying the optimal elicitor or combination for broad polyphenol production remains critical (Ahmad *et al.,* 2017). Biotic elicitors are derived from biological sources, such as polysaccharides from plant cells and microbial walls (Goyal *et al.,* 2012). In contrast, abiotic elicitors encompass physical and chemical stressors, including exposure to metal ions, inorganic compounds, UV light, or electric currents (He *et al.,* 2018). Inducing secondary metabolites by activating stress signaling pathways represents a promising approach to boosting their production in plant cell cultures.

Methyl jasmonate (MeJA) plays a significant role in plant defenses against herbivores and pathogens by acting as signaling molecule (Yang *et al.,* 2015; Hall *et al.,* 2020). It has been shown to boost the accumulation of secondary metabolites with antioxidant properties (Ali *et al.,* 2015). Fungal elicitors derived from fungal cell wall components have also been shown to enhance secondary metabolite production in plant cultures (Naik *et al.,* 2016).

Previous studies have indicated that specific polyphenols, including indole alkaloids such as ajmalicine, catharanthine, and serpentine, significantly increase in *Catharanthus roseus* cell suspensions when elicited with fungal agents (Liang *et al.,* 2018; Mueed *et al.,* 2023; El-Saadony *et al.,* 2024b). Similarly, cultures of *Rauwolfia canescens* treated with fungal elicitors showed substantial increases in 12-oxophytodienoic acid and raucaffrincine production. Yeast extract (YE) is another effective elicitor,

particularly known for enhancing silymarin accumulation (Sánchez-Sampedro *et al.,* 2005a; Elwekeel *et al.,* 2012). Treatment with YE can led to an increase in the production of silymarin (upto threefold) and release into the culture medium compared to untreated controls (Sánchez-Sampedro *et al.,* 2005b).

Silymarin had protective effects against renal damage and oxidative stress in male rats induced by diclofenac (Nouri and Heidarian, 2019). Silybum marianum total extract, silibinin, and silymarin mitigated renal carcinogenesis in Wister rats by modulating various mechanisms including apoptosis, oxidative stress, PI3K/AKT signaling pathways and NF-κB (Yassin *et al.,* 2021). However, there are no available studies about inducing silymarin content in cell suspension cultures of *Silybum marianum* L., then using the silymarin-enriched extract (SME) on oxidative stressed rats by $HgCl_2$. The primary objectives of this study were to: (1) examine the effects of methyl jasmonate (MeJA) and yeast extract (YE) elicitors on enhancing silymarin production in *Silybum marianum* L. cell suspension cultures, (2) quantify and characterize the silymarin components using HPLC analysis, and (3) evaluate the extract's biological activities including antidiabetic, antimicrobial, anticancer, antioxidant and neuroprotective properties. Additional objectives focused on assessing the hepatoprotective effects of the silymarin-enriched extract against $HgCl_2$-induced toxicity in rats by analyzing liver function markers, inflammatory cytokines, apoptotic factors, and gut microbiota composition. The study also aimed to compare the efficacy of MeJA versus YE for silymarin production and establish correlations between silymarin content and bioactivity, ultimately proposing the extract as a potential multifunctional therapeutic agent for oxidative stress-related disorders.

MATERIALS AND METHODS

In Vitro Germination for Explant Source

Initiation of Tissue Culture: Surface-sterilized seeds were germinated *in vitro* on Murashige and Skoog (MS) medium supplemented with 30 gm/L sucrose and 8 g/L agar (**Table 1**). Seedlings were grown under controlled conditions (25°C, 16 h light/8 h dark photoperiod) for four weeks, providing explants (root segments, hypocotyls, and leaves) for callus induction.

Callus Induction and Proliferation: MS medium supplemented with sucrose (30 g/L), agar (8g/L) were used to culture explants and varying combinations of kinetin (0, 0.5, 1, and 1.5 mg/L) and 2,4-dichlorophenoxyacetic acid (2,4-D) (0, 0.25, 0.5, and 1 mg/L). Callus cultures were subcultured on fresh MS medium every three weeks with the same PGR composition (**Table 1**). Control media lacked PGRs.

Elicitor Treatment for Enhanced Silymarin Production: Selected callus cultures were treated with yeast extract (1, 2, and 4 mg/L) or methyl jasmonate (100, 200, and 400 µM) to enhance silymarin production (Sánchez-Sampedro et al., 2008). Elicitors were added to the medium, and cultures were subcultured every two weeks on fresh MS medium containing the same PGRs and elicitors. Control cultures lacked elicitors. Each experimental setup was replicated three times.

Initiation of Cell Suspension Culture: Root explants (friable calli) with high silymarin content were used to start cell suspension cultures. Calli (~10 g fresh tissue) were fragmented (~0.5 g pieces) and transferred to flasks containing 50 mL of liquid MS medium (4.4 g/L) supplemented with 30 g/L sucrose, 1.5 mg/L kinetin, and 1 mg/L 2,4-D (pH 5.8). Cultures were sustained in darkness at 27°C on a rotating platform (130 rpm). After four days, the volume was increased to 100 mL with fresh medium. Subculturing was performed every 7-10 days (30 mL cell suspension to 70 mL fresh medium).

Elicitor Treatments in Cell Suspension: Cell suspension cultures were treated with methyl jasmonate (100 µM) or yeast extract (4 mg/L) (Widholm, 1972), which corresponds to the optimal elicitor concentrations found in callus cultures. Elicitors were added three days post-transfer, and control cultures lacked elicitors. The growth index [(Final cell FW - Initial cell FW) / (Final initial cell FW)] and cell viability (fluorescein diacetate staining) (Cacho *et al.,* 1999) were assessed. All cultural experiments were performed in triplicate.

Preparation of *Silybum marianum L.* Cultures Extract: Callus and cell suspension cultures were dried at 50 °C, ground into powder, and extracted with 200 mL of 70% aqueous ethanol using a thermo-shaker (38 °C, 180 rpm) for two hours (Aytul, 2010). The extracts were centrifuged (5000 ×g, 20 min), the solvent was evaporated (38 °C, 120 rpm), and the remaining aqueous extract was lyophilized (-60 °C, 0.028 Mbar) to obtain a powder for further analysis. This procedure yielded a homogenous powder to analyze silymarin content and biological activities.

Table 1: The Composition of Nutrient Media Used in Different Stages of this Study

Medium	Composition
	Stage 1
M	4.4gm/L MS + 30 gm/L sucrose + 8 gm/L agar
M1	4.4gm/L MS + 0.5mgLl Kin+ 0.25mg/L 2,4 D + 30gm/L sucrose + 8 gm/L agar
M2	4.4gm/L MS + 1mg/L Kin+ 0.5mg/L 2,4 D + 30gm/L sucrose + 8gm/L agar
M3	4.4gm/L MS + 1.5mg/L Kin+ 1mg/L 2,4 D + 30gm/L sucrose + 8gm/L agar
	Stage 2
M4	M3 + 100 µM /L of Methyl jasmonate
M5	M3 + 200 µM /L of Methyl jasmonate
M6	M3 + 400 µM/L of Methyl jasmonate
M7	M3 + 1mg /L of yeast extract
M8	M3+ 2mg /L of yeast extract
M9	M3+ 4mg /L of yeast extract
	Cell suspension
M10	M4 (without agar) liquid
M11	M9 (without agar) liquid

Characterization of SME

Phenolic Compounds Profile: The total phenolic content was measured using the Folin-Ciocalteu method, as outlined by Saad *et al.* (2021). Flavonoids and phenolic compounds were analyzed using a Shimadzu HPLC (Japan) equipped with a UV-Vis DAD detector. Gemini C18 column with a flow rate of 0.5 mL/min at a

temperature of 5 °C was used to separate polyphenols. The SME was dissolved in a 50:50 methanol-water mixture and injected into the autosampler. All chemicals used were of HPLC grade, including phosphoric acid and acetonitrile, combined with water (Carlo Erba) to achieve a pH of 2. A total runtime of sixty minutes was utilized, with a gradient elution profile changing as described by Alharbi *et al*., (2024).

Antidiabetic activity: The SME inhibition activity of α-glucosidase was evaluated calorimetrically as follows. SME concentrations (100, 150, and 200 µg/mL) were incubated with α-glucosidase at pH 6.9 and 37°C for 10 min. Then, 50 µL of a 1 mM p-NP-α-D-glucopyranoside solution (in PBS) was added, and the reaction was terminated after 10 min. The OD was then read at 405 nm and applied to the equation (Carneiro *et al.,* 2022). α-Amylase inhibitory activity was assessed following the method of Nair et al. (2013).

$$\%\ \alpha - glucosidase\ inhibition\ activity = \frac{OD\ control - OD\ sample}{OD\ control}\ x\ 100$$

Antioxidant Activity: The DPPH scavenging activity of SME was assessed according to Abdel-Moneim *et al.* (2022). A reaction between 0.5 mL of ethanolic DPPH and 1 mL of SME was incubated in the dark for 30 min, and the absorbance at 517 nm was measured spectrophotometrically. The IC_{50} value reflects the minimum concentration required to scavenge 50% of the DPPH radical (Al-Quwaie et *al.,* 2023).

$$\%\ DPPH\ scavenging\ activity = \frac{Abs\ control - Abs\ sample}{Abs\ control}\ x\ 100$$

Antimicrobial Activity: The antibacterial properties of SME were tested against *Salmonella* Typhi*, Bacillus cereus,* and *Candida albicans*. The antibacterial potential of the SME was evaluated using the agar well-diffusion method as described by Al-Quwaie et *al.* (2023). After adding 50 mL of melted Muller-Hinton agar (MHA) to the plates, a loopful of bacterial inoculum was evenly distributed across the surface of each plate. Each plate was punctured with 8 mm wells, into which 6 mm discs soaked with 50 µL SME at levels of 100, 150, and 200 µg/mL were added. Negative control wells contained discs with water. MHA plates were then incubated for 24–48 h at 37 °C. The diameters of inhibition zones (mm) were measured to indicate antibacterial activity.

The antifungal potential of SME concentrations (100, 150, and 200 µg/mL) was tested against pathogenic fungi: *Fusarium oxysporium, Fusarium oxysporium, Fusarium solai, Rhizoctonia solani, Aspergills niger, Alternaria alternata, Pythium aphanidermatum,* and *Botrytis cinerea*. A disc diffusion assay was employed to assess the SME's antifungal activity (Alsubhi *et al.,* 2022). The fungal suspensions were cultured on Sabouraud dextrose agar plates. Sterile paper discs impregnated with various SME concentrations were placed on the inoculated Sabouraud dextrose plates at 28 °C for 7 days. Zones of inhibition were measured in mm.

Antiviral activity

Virus and cells: The strains of human parvovirus B19 and Sapporo viruses were obtained from the American Type Culture Collection (ATCC). For *in vitro* experiments, Vero (African green monkey kidney) and BHK-21 (baby hamster kidney) were procured from ATCC. Eagle's Minimum Essential Medium (EMEM; Gibco, NY, USA) supplemented with 10% heat-inactivated fetal bovine serum (FBS) and penicillin-streptomycin, under standard incubation conditions (37°C, 5% CO_2) was used to maintain both cell lines.

Cell Viability Assay: The cytotoxicity of the SME against Vero and BHK-21 cells was evaluated using the MTS assay (Promega). Briefly, cells grown in 96-well plates were treated with varying concentrations of each compound (in triplicate) and a 0.1% DMSO control. After 48 hours of incubation at 37°C with 5% CO_2, MTS solution was added, and absorbance was measured at 495 nm using a Tecan Infinite 200 Pro reader after a 4-hour incubation. All experiments were performed in triplicate, and the half-maximal cytotoxic concentration (CC_{50}) was determined.

Antiviral Activity Assay:

Primary Assay: Vero cells were grown in 96-well plates with EMEM containing 2% FBS. SME, human parvovirus B19 and Sapporo viruses (multiplicity of infection, MOI=1) were added in triplicate. Following a 48-hour incubation at 37°C with 5% CO_2, cytopathic effect (CPE) was assessed microscopically and expressed as a percentage of the virus control. The results were confirmed using the MTS assay (Promega), in triplicates.

Anticancer Activity

Cytotoxicity assay: The SRB assay assessed cell viability using Hepatocellular carcinoma cell line (HepG2) as described by Khojali *et al.,* (2023).

$$Cell\ viability\ (\%) = \frac{\text{absorbance of the sample} - \text{absorbance of the blank}}{\text{absorbance of the control} - \text{absorbance of the blank}}\ \text{x}\ 100$$

Anti-Alzhaimar activity: Acetylcholinesterase activity was estimated by Quanti-Chrome assay kit (USA) using a 96-well plate reader (El-Hawwary *et al.,* 2021). The enzyme hydrolyzes acetylthiocholine, generating thiocholine. This product reacts with 5,5'-dithiobis (2-nitrobenzoic acid) (DTNB), forming 5-thio-2-nitrobenzoate (yellow color), which was read at 412 nm, and was directly proportional to the enzyme activity in the samples.

***In vivo* Experiment:** One hundred twenty male Wistar Albino Rats (Rattus norvegicus Bork) weighing 180-190 g were obtained from a breeding facility, acclimatized, and maintained under hygienic conditions. The rats were housed in plastic cages on a 12-hour light-dark cycle, with a relative humidity of 40-60%, a temperature of 23.2 °C, and had unlimited access to water and a standard diet throughout the study (NRC, 1996). Following a two-week acclimatization period, the animals were weighed and randomly assigned to four groups: G1 received the basal diet, G2 was the $HgCl_2$-challenged group, G3 was treated

with SME (200 mg/kg diet), and G4 was fed the HgC_{l2}-challenged diet and treated with SME (200 mg/kg diet).

Mercuric chloride ($HgCl_2$) was strategically selected as the model toxin in this study due to its well-documented ability to induce systemic toxicity across multiple organ systems, making it an ideal candidate for evaluating the comprehensive protective effects of the silymarin-enriched extract (SME). As a heavy metal compound, $HgCl_2$ induces robust oxidative stress through glutathione depletion and lipid peroxidation, particularly in the liver where it significantly elevates ALT and AST levels while upregulating pro-inflammatory cytokines (IL-1β and TNF-α). Its effects extend to the gastrointestinal system, where it disrupts the gut microbiome by reducing beneficial bacterial populations while promoting pathogenic species, concurrently compromising intestinal barrier integrity and facilitating endotoxin translocation. Notably, $HgCl_2$'s ability to cross the blood-brain barrier allows it to induce neurotoxic effects characteristic of heavy metal exposure, including acetylcholinesterase hyperactivity and oxidative damage in neural tissues. This multi-organ toxicity profile makes $HgCl_2$ particularly valuable for assessing SME's purported hepatoprotective, gut-modulatory, and neuroprotective properties in a single experimental model. Furthermore, $HgCl_2$-induced toxicity closely mimics pathological features of environmental heavy metal exposure in humans, enhancing the translational relevance of the findings (Makena *et al.,* 2022).

Blood Biochemistry: At the end of 28 days, the rats were fasted overnight and then euthanized via jugular vein severance, and two blood samples were collected. The first 0.5 mL sample was placed in an EDTA tube for hematological analysis. The second 2 mL sample was collected in EDTA-free tubes, centrifuged at 3000 rpm for 10 minutes to isolate the serum, and stored at -20 °C until biochemical tests were performed within two weeks (Cadamuro *et al.,* 2018). Serum levels of aspartate transaminase (AST), alanine transaminase (ALT), and alkaline phosphatase (ALP) were measured using a colorimetric technique. ALP levels were determined according to the method described by Belfield and Goldberg (1971). Total serum protein concentrations were measured, while albumin levels were analyzed using the method described by Westgard and Poquette (1972). Serum globulin was calculated by subtracting the albumin level from total protein.

Proinflammatory and precancerous relative gene expression: Total RNA was extracted following the method described by Dong *et al*. (2020). The isolated RNA was subsequently used for quantitative real-time PCR (qRT-PCR) analysis. All qRT-PCR reactions were performed using SYBR Green chemistry on a real-time PCR system. Melting curve analysis was performed to ensure the specificity of the PCR product. Gene-specific primers for Bax, Caspase 3, IL-β1, and IL-6 were used for quantitative real-time PCR (qRT-PCR). The 2-ΔΔCt method was used to determine relative gene expression (Livak and Schmittgen, 2001).

Histopathology: Liver and intestinal samples were collected, preserved in formalin, and processed using an automated histological processor. The tissues were immersed in a 10% formalin solution for 48 hours, then rinsed with distilled water for 30 min. Dehydration was performed by increasing alcohol concentrations (70, 90, and 100%) for 120 minutes each, followed by additional immersion in xylene. Finally, the specimens were fully impregnated with molten paraffin wax and sealed. Hematoxylin and eosin staining was used on paraffin-embedded tissue sections 4-5 µm thick (Suvarna and Niranjan, 2013).

Intestinal Microbial Counts: After the rats were euthanized, intestinal digesta was collected and mixed in sterile glass containers, which were then stored at 4°C prior to microbial enumeration. The microbial population was analyzed for total bacterial count, *E. coli*, TYMC, and *Lactobacillus* spp., using selective media as described by Abd El-Wahab *et al.* (2022). Counts were converted to log CFU/g of digesta.

Statistical Analysis: The means of triplicate data were analyzed using one-way analysis of variance (ANOVA) to evaluate the treatment effects and potential interactions on the measured outcomes. Before performing ANOVA, the homogeneity of variance was confirmed. Following significant ANOVA results ($P<0.05$), the LSD post-hoc test was applied for multiple group comparisons. All analyses were performed using statistical software (SPSS v 21, IBM, USA).

RESULTS

Callus Induction: The initiation of callus in *S. marianum* L. is greatly affected by the types and concentrations of plant growth regulators (PGRs) in the culture medium. Table 2 outlines that varying concentrations of 2,4-D and kinetin (Kin) impact callus development from different explants, including roots, hypocotyls, and leaves (as depicted in Fig. 1). No callus formation noted on the control MS basal medium. The combination of 2,4-D and Kin had a positive effect on callus induction after 70 days of cultivation (Table 2). A two-way ANOVA identified a significant interaction ($P<0.05$) between the levels of kinetin and 2,4-D for callus formation across all explant types (roots, hypocotyls, leaves), with an increase in the concentrations of both PGRs enhancing callus production from root explants (Table 2).

Callus Biomass Yield and Silymarin Production (Stage 1): The callus derived from root explants exhibited the greatest ability to produce silymarin when cultured on MS medium supplemented with 1 mg/L 2,4-D and 1.5 mg/L Kin (Table 2). Similarly, the leaf explants yielded the highest silymarin concentration on a medium containing 0.5 mg/L 2,4-D and 1 mg/L Kin. Likewise, hypothotyl explants exhibited peak silymarin accumulation with the same concentrations (0.5 mg/L 2,4-D and 1 mg/L Kin) (Fig. 1). The two-way ANOVA results indicated a significant correlation ($P<0.05$) between the explant type and the levels of 2,4-D/Kin, as observed in fresh and dry callus, and the weights of silymarin content. The explant type and its interaction with PGR concentrations significantly impacted these metrics ($P<0.05$). Control cultures were maintained in the same medium as the treatment groups, but without any

PGR. All experimental cultures were conducted in triplicate. When comparing explant types, root explants produced callus with significantly greater fresh and dry weights, preferred texture and color, higher callus induction frequency, and total silymarin content (Table 2). Root explants treated with 1 mg/L 2,4-D and 1.5 mg/L Kinetin produced the highest callus induction (98%), fresh weight (4.45 g), dry weight (0.2673 g), and silymarin content (0.527 µg/mL), making them the best treatment for callus growth and silymarin production.

Callus Biomass Yield and Silymarin Production (Stage 2): In this stage, we examined the effects of elicitors on callus growth and silymarin production (Fig. 2). The root explants, which yielded the highest silymarin content in Stage 1, were treated with methyl jasmonate and yeast extract to assess their elicitor effects. The optimal concentrations for each elicitor were 100 µM/L for methyl jasmonate and 4 mg/L for yeast extract. Table 3 summarizes the effects of elicitors on fresh weight, dry weight, texture, color, callus induction frequency, and overall silymarin content in the callus culture. MeJA at 100 µM/L was the most effective treatment for increasing silymarin production (0.912 µg/mL) in root explants, despite having a lower fresh and dry weight than YE treatments.YE treatments (especially at 1 mg/L and 2 mg/L) resulted in the highest fresh and dry weights. However, their impact on silymarin yield was lower than that of MeJA.The control treatment with no elicitor showed the highest callus induction rate (98%). The lowest silymarin yield, indicating that while the PGRs alone were effective for callus induction, adding elicitors like MeJA and YE enhances the production of valuable metabolites (like silymarin) without severely affecting callus induction. The MeJA treatments, especially at 100 µM, offer the best balance for enhancing silymarin production; meanwhile, YE treatments provide the highest fresh and dry weights, making them suitable for improving biomass production.

Elicitor Treatments: The treatment duration significantly influenced cell growth, with a decline phase starting 72 hours post-treatment. An exponential growth phase was observed between 24 and 48 hours, during which rapid cellular proliferation occurred, peaking in dry weight at the end of 48 hours. Table 4 outlines the results for dry cell weights and total silymarin content from cell suspensions treated with elicitors compared to control samples. After 24 hours of treatment, cells exposed to MeJA and YE recorded dry weights of 1.567 g and 1.4473 g DW, alongside total silymarin contents of 0.962 µg/mL and 0.867 µg/mL, respectively. This increased to maximum values after 48 hours, reaching 1.899 g and 1.859 g for dry cell weight,

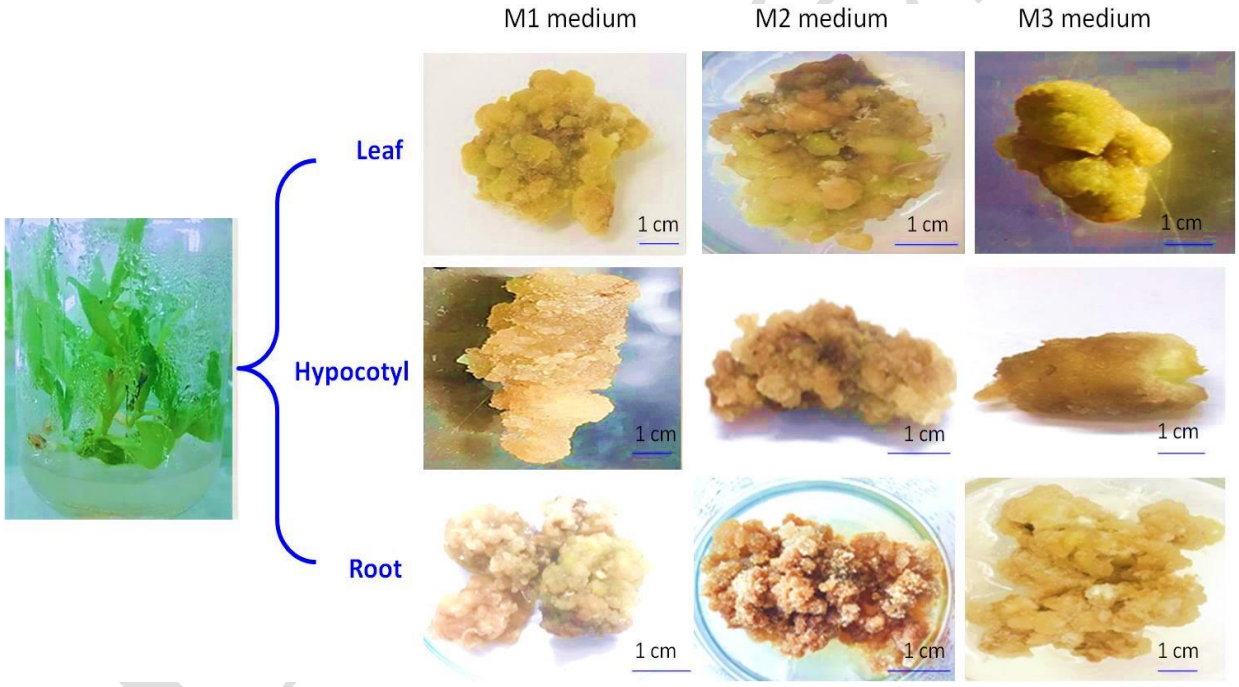

Fig. 1: Establish callus cultures using three explant types (Leaf, Hypocotyls, and Root) of S. *Marianum* L. on three types of MS media. scale 1cm.

Table 2: Effects of Plant Growth Regulators (kinetin and 2,4-D) on Fresh Weight, Dry Weight, Texture, Color, Callus Induction Frequency, and Total Silymarin Content from the Callus Culture Derived from Using Various Explant Types of *S. Marianum L.*

Explant	PGR (mg/L) 2,4-D	Kin	Callus Induction (%)	Texture and color of Callus	Fresh Weight (gm)	Dry weight (gm)	Silymarin (µg /ml) (DW)
(Control)	0.0	0.0	0	_____	No callus induction	No callus induction	0.224
Leaf	0.25	0.5	93	Greenish Yellow Friable	1.4133 ^{h}	0.1193^{c}	0.147
Leaf	0.5	1	90	Greenish Yellow Friable	1.6267 ^{g}	0.1223^{c}	0.172
Leaf	1	1.5	94	Greenish Yellow Friable	3.5233 ^{b}	0.2420^{a}	0.194
Hypocotyl	0.25	0.5	90	Yellowish Creamy Friable	1.12 ^{i}	0.0783^{d}	0.148
Hypocotyl	0.5	1	92	Yellowish creamy Friable	2.62 ^{d}	0.1221^{c}	0.187
Hypocotyl	1	1.5	95	Yellowish Creamy Friable	2.3333 ^{e}	0.1297^{c}	0.254
Root	0.25	0.5	97	Yellowish Creamy Friable	1.94 ^{f}	0.1277^{c}	0.326
Root	0.5	1	93	Yellowish Creamy Friable	3.22 ^{c}	0.1873^{b}	0.433
Root	1	1.5	98	Yellowish Creamy Friable	4.45^{a}	0.2673 ^{a}	0.527

Significant differences are indicated using distinct letters (P<0.05) based on the LSD test.

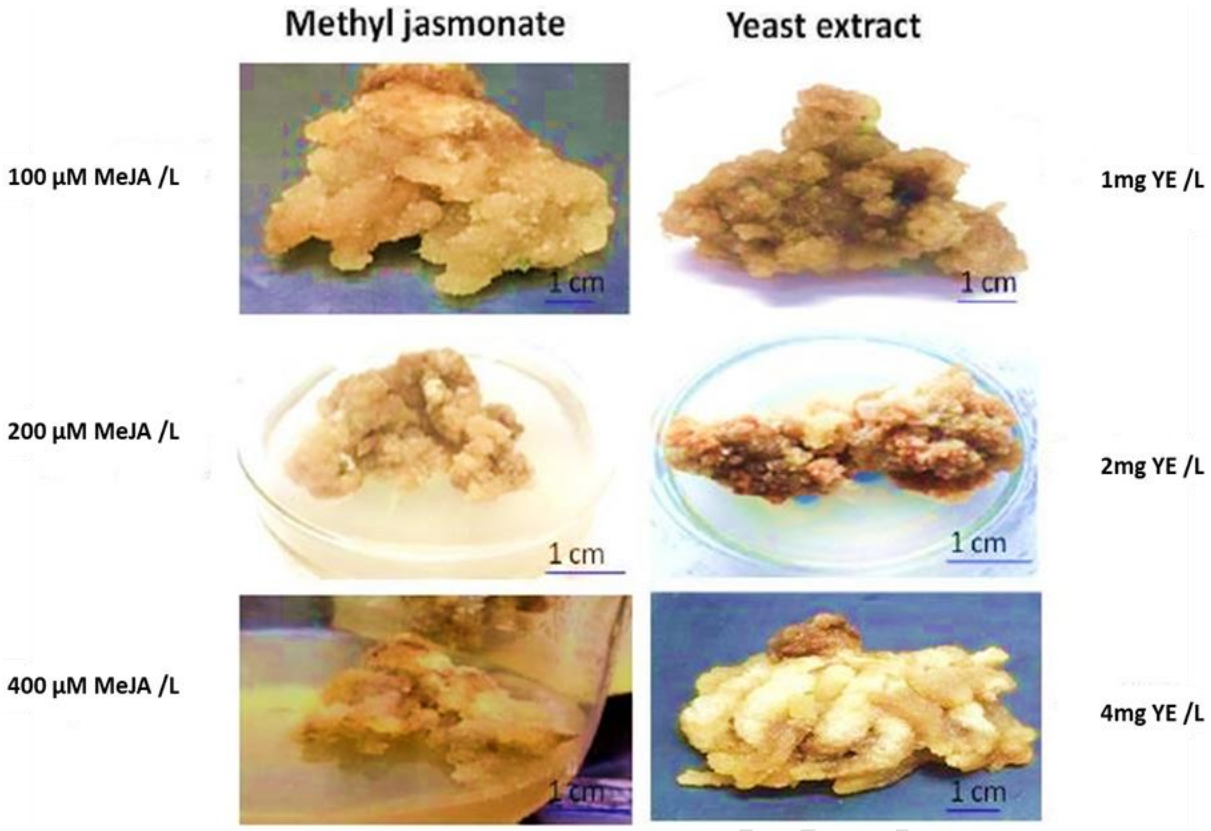

Fig. 2: Effect of different concentrations of methyl jasmonate and yeast extract *in vitro* roots-derived callus on MS medium with M3.

Table 3: The Effect of Different Concentrations of Methyl Jasmonate (MeJA) and Yeast Extract (YE) on Fresh Weight, Dry Weight, Texture, Color, Callus Induction Frequency, and Total Silymarin Content from the Callus Culture Derived from the Root Explants of *S. Marianum* L.

Explant	Elicitor concentrations	PGR (mg/L) 2,4-D	Kin	Callus Induction (%)	Texture and color of Callus	Fresh weight (g)	Dry weight (g)	Silymarin (µg /ml DW)
Control (Root)		1	1.5	98	Yellowish Creamy Friable	4.45 ^{a}	0.2673^{d}	0.527
Root	100 µM /L MeJA	1	1.5	92	Yellowish Creamy Friable	3.3061^{c}	0.4653^{c}	0.912
Root	200 µM /L MeJA	1	1.5	93	Yellowish Creamy Friable	3.5032^{c}	0.4653^{c}	0.845
Root	400 µM /L MeJA	1	1.5	96	Yellowish Creamy Friable	3.4234^{c}	0.3193^{d}	0.832
Root	1mg YE /L	1	1.5	90	Yellowish Creamy Friable	4.6017^{a}	0.8823^{b}	0.702
Root	2mg YE /L	1	1.5	92	Yellowish Creamy Friable	4.152^{b}	1.1223^{a}	0.734
Root	4mg YE /L	1	1.5	94	Yellowish Creamy Friable	4.162^{b}	1.183^{a}	0.782

Significant differences are indicated using distinct letters (P<0.05) based on the LSD test.

Table 4: Effect of Methyl Jasmonate (100 µM/L) and Yeast Extract (4 mg/L) Application on the Cell Dry Weight (g) and Silymarin Content (µg/ml DW) in *Silybum marianum* L.cell Suspension Culture

Time (hours)	Elicitor concentrations	Cell dry weight (gm)	Silymarin (µg /ml DW)
24h	Control	1.121^{de}	0.701
	100 µM MeJA /L	1.567^{b}	0.962
	4mg YE /L	1.4473^{bc}	0.867
48h	Control	1.124^{de}	0.743
	100 µM MeJA /L	1.899^{a}	1.0728
	4mg YE /L	1.859^{a}	1.0526
72h	Control	0.9867^{e}	0.721
	100 µM MeJA /L	1.277^{cd}	1.0517
	4mg YE /L	1.326^{cd}	1.0214

Significant differences are indicated using distinct letters (P<0.05) based on the LSD test.

1.0728 µg/mL and 1.0526 µg/mL DW for total silymarin. MeJA (100 µM) is the most effective elicitor for cell dry weight and silymarin production. It consistently produced the highest cell dry weight and silymarin content at 48 and 24 h, highlighting its potential to enhance cell growth and secondary metabolite production. YE (4 mg/L) also showed promising results, particularly at the 48-h point, reaching a cell dry weight almost comparable to that of MeJA; however, its overall effectiveness in silymarin production was somewhat lower than that of MeJA.The control group exhibited cell growth and silymarin production, but these levels were lower than those obtained with MeJA and YE treatments, particularly after 48 hours. As a result, both MeJA and YE effectively promoted cell growth and silymarin production, with MeJA demonstrating a greater overall efficacy, especially in the initial phases of the experiment.

Total Phenolic Content of *S. marianum* Extracts: Table 5 presents the total phenolic content (TPC) of different extracts obtained from cell and callus cultures of *S. marianum* L. The results indicate how variations in the concentrations of plant growth regulators (PGRs) or elicitors impact TPC. There was notable variability in phenolic content among the analyzed extracts, with those exhibiting the highest TPC values being particularly notable. Fig. 3 shows that MeJA treatments, especially at a medium concentration of 100 µM, led to the highest silymarin yield. Table 5 presents that A4: (MeJA treatment at 100 µM) demonstrated the highest TPC value at 321.61, whereas A3: (MeJA treatment at a concentration of 100 µM during stage 2) showed a TPC value of (280.25).

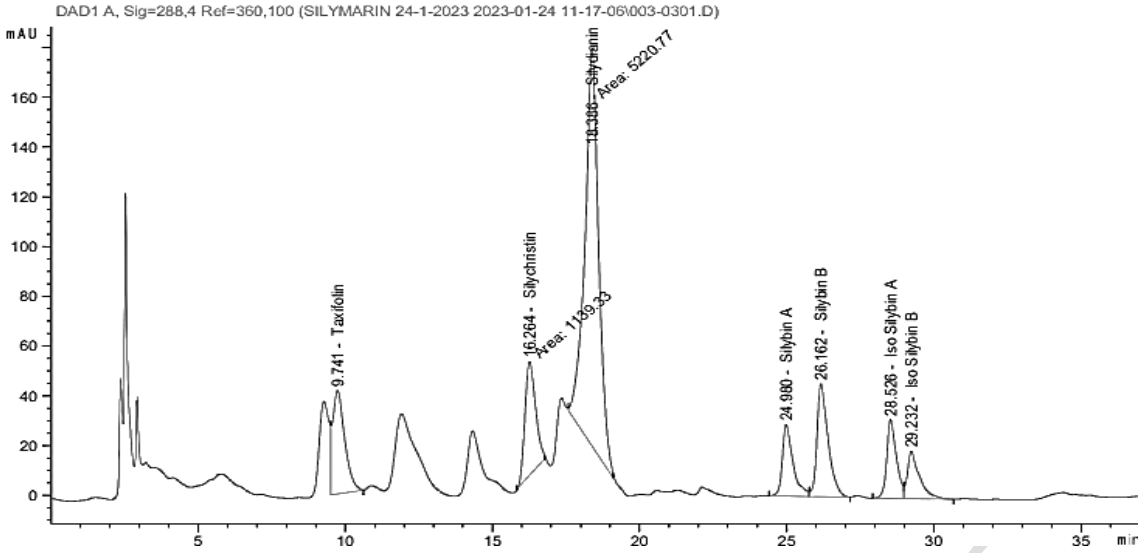

Fig. 3: An analysis of silymarin was performed using HPLC on extract from M10 medium.

Table 5: Polyphenolic amount (mg/g), antioxidant, and anticancer activity of four selected samples

Samples	TPC	Antioxidant activity (%)	Anticancer activity IC_{50} (µg/mL)
A1	191.13	45	55.3
A2	201.55	60	49.8
A3	280.25	88	22.5
A4	321.61	96	18.1

A1: Callus derived from the root explants on M medium. A2: Callus derived from the root explants on M3 medium. A3: Callus derived from the root explants on M4 medium. A4: Callus derived from the root explants on M10 medium.

Table 6: Silymarin profile detected by HPLC

Content	A1	A2	A3	A4
Silydianin	18^{c}	24^{ab}	22^{b}	26^{a}
Silychristin	10^{d}	49^{b}	23^{c}	55^{a}
Silymarin	160^{d}	301^{b}	240^{c}	320^{a}
Taxifolin	19^{c}	33^{ab}	28^{b}	35^{a}
SilibininA	45^{b}	66^{a}	32^{c}	66^{a}
SilibininB	62^{b}	89^{a}	45^{c}	68^{b}
IsosilibininA	15^{b}	22^{a}	15^{b}	17^{b}
IsosilibininB	4^{b}	6^{ab}	5^{b}	8^{a}

Lowercase letters in each row significantly indicated the differences between treatments

Table 6 and Fig. 3 stated that SM Extract of root-derived callus produced on M3 + 100 µM /100ml of methyl jasmonate optimized the high content of silymarin (flavonolignans mixture), where Silibinin A and B accounted for 0.134 mg/g SME, Isosilibinin A and B accounted for 0.025 mg/g. The silymarin content was 0.3 mg/g after treating the SM callus with MJ.

Biological Activities

Antidiabetic activity: Fig. 4 shows the inhibition activity of SME on two enzymes: α-amylase and α-glucosidase. Here's a breakdown of the data: Fig. 4A shows that SME at 200 µg/mL inhibited 81% of α-amylase activity; as the SME concentration increases, the inhibition of α-amylase activity also increases. Also, in Fig. 4B, Similar to α-amylase, the inhibition of α-glucosidase activity increases with higher SME concentrations, where SME at 200 µg/g reduced the activity of α-glucosidase by 75 %.

For both enzymes, the inhibitory effect of SME is dose-dependent. Higher concentrations of SME lead to greater inhibition of enzyme activity. The inhibition trends for both α-amylase and α-glucosidase are pretty similar, suggesting that SME might have a general inhibitory effect on both enzymes, possibly through a common mechanism.

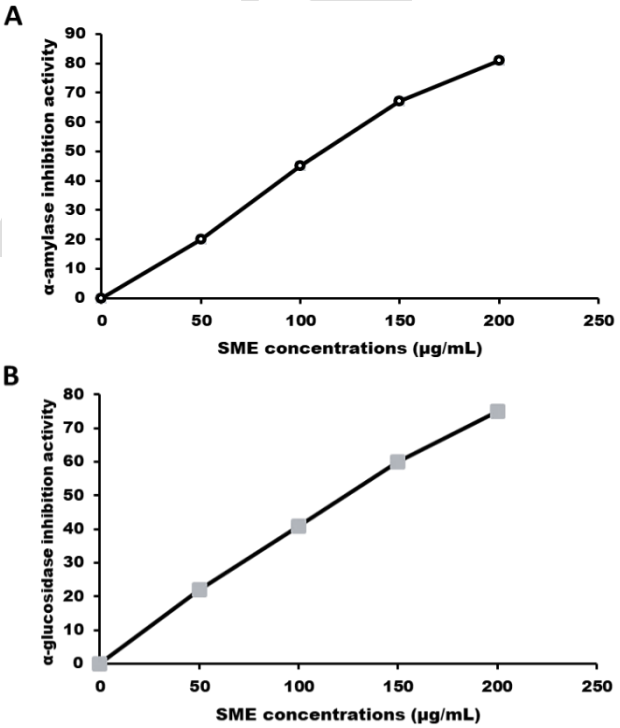

Fig. 4: Antidiabetic activity of silymarin enriched extract against (A) α-amylase activity and (B) α-glucosidase activity.

Antioxidant Activity: The antioxidant activity of extracts from selected high-silymarin cell and callus samples was evaluated using the stable DPPH radical. The data in Table 5 demonstrate the significant antioxidant capacity of the SME from the four samples tested, all of which show substantial antioxidant activity. Notably, elicitor treatments resulted in greater antioxidant effects in *Silybum marianum* (L.) compared to treatments with PGRs. While all samples were assessed, Table 5 presents result specifically for the best-performing samples, where the A4: (MeJA treatment at 100 µM) exhibited the highest antioxidant activity (96%), while A3: (MeJA treatment at a concentration of 100 µM during stage 2) demonstrated an activity level of 88%.

Anticancer Activity: The SME exhibited anticancer properties against human Hepatocellular carcinoma cells, as illustrated in Table 5 and Fig. 5. These findings align with microscopic evaluations. Furthermore, Fig. 5 illustrates an inverse relationship between the IC_{50} values of treatments and their percentage inhibition. The IC_{50} values of the chosen samples were compared to those of doxorubicin in Table 5. A4 is the sample with the best overall results, having the lowest IC_{50}, indicating the most potent anticancer activity. Based on these findings, A4 is considered the most effective in terms of antioxidant and anticancer activity compared to the other samples. IC_{50} is the concentration required to inhibit 50% of cancer cell growth; the lower the IC_{50} value, the stronger the anticancer activity. A4: (MeJA treatment at 100 µM) has the lowest IC_{50} value (18.1 µg/mL), indicating the most potent anticancer activity, followed by A3: (treatment with MeJA at a concentration of 100 µM during stage 2), which demonstrated an anticancer activity value of 22.5 µg/mL.

Antimicrobial Activity: As shown in Table 7 and Fig. 6, SME significantly inhibited the growth of pathogenic bacteria. Among the tested microorganisms, *E. coli* showed the most resistance, with an inhibition zone of 25-29 mm across all treatments, followed by *C. albicans. B. cereus* was the most susceptible bacterium to the tested samples. A4 consistently showed the largest inhibition zone diameter, indicating it has the most potent antibacterial and antifungal activity compared to the other samples. A4: (MeJA treatment at 100 µM) is the sample that achieved the best results across all targeted organisms (*B. cereus, E. coli,* and *C. albicans*) and at all concentrations.

The antifungal efficacy of SME was tested against phytopathogenic fungi, including *Fusarium oxysporum, F. solani, Aspergillus niger, Alternaria alternata, Pythium aphanidermatum,* and *Botrytis cinerea*. Inhibition zone diameters (IZDs) increased proportionally with SME concentration, ranging from 18 to 39 mm. The 150 µg/mL SME concentration exhibited the strongest antifungal activity. *P. chrysogenum, F. oxysporuim, A. alternata,* and *B. cinerea* demonstrated the highest resistance, showing the smallest inhibition zones. At the highest SME concentration, IZDs ranged between 32 and 39 mm (**Fig 7**).

Antiviral activity: The cytotoxicity evaluation of milk thistle extract (SME) in Vero and BHK21 cell lines demonstrated excellent safety parameters, with a half-maximal cytotoxic concentration (CC_{50}) exceeding 150 µg/mL in both cell types, indicating low cellular toxicity at therapeutic concentrations. In antiviral testing against human parvovirus B19 (PVB-19), SME exhibited potent dose-dependent inhibition, achieving 89% reduction in cytopathic effects at the highest tested concentration (100 µg/mL), with a calculated half-maximal inhibitory concentration (IC_{50}) of 32 µg/mL. Similar vigorous activity was observed against Sapporo virus (SaV), where SME treatment resulted in 76% inhibition of viral cytopathology at 100 µg/mL and an IC_{50} of 45 µg/mL (Table 8). The selectivity indices ($SI=CC_{50}/IC_{50}$), a key indicator of therapeutic window, were determined to be 4.7 for PVB-19 and 3.3 for SaV, suggesting favorable efficacy-to-toxicity ratios for both viral targets. Confirmatory MTS viability assays validated these findings, showing SME treatment restored cell viability to 82% in PVB-19-infected cultures and 71% in SaV-infected cultures compared to untreated infected controls (Table 8). These results demonstrate that SME maintains robust antiviral activity while preserving host cell viability, with powerful effects against PVB-19. The dose-response patterns observed in both CPE and MTS assays indicate that SME's antiviral mechanism likely involves interference with viral replication or cell entry processes, consistent with its reported activity against other enveloped viruses. The reproducibility of these effects across three independent experimental replicates confirms the reliability of SME's antiviral properties against these clinically relevant pathogens.

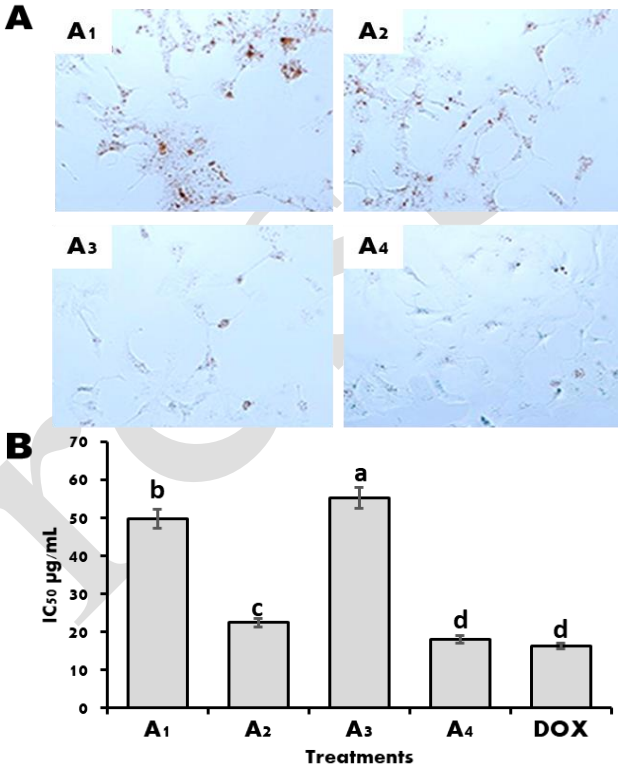

Fig. 5: A) Microscopic image of the antiproliferative activity of SME. A1: callus derived from the root explants on M medium. A2: callus derived from the root explants on M3 medium. A3: callus derived from the root explants on M4 medium. A4: callus derived from the root explants on M10 medium. B) The IC_{50} of SME against the cancer cell lines compared to doxorubicin (DOX). Lowercase letters above columns indicate significant differences $P<0.05$.

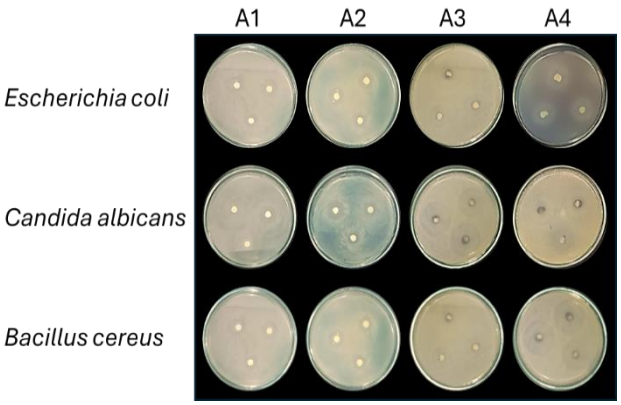

Fig. 6: Illustration of the Antimicrobial Effects of the Four Selected Samples. A1: callus derived from the root explants on M medium. A2: callus derived from the root explants on M3 medium. A3: callus derived from the root explants on M4 medium. A4: callus derived from the root explants on M10 medium.

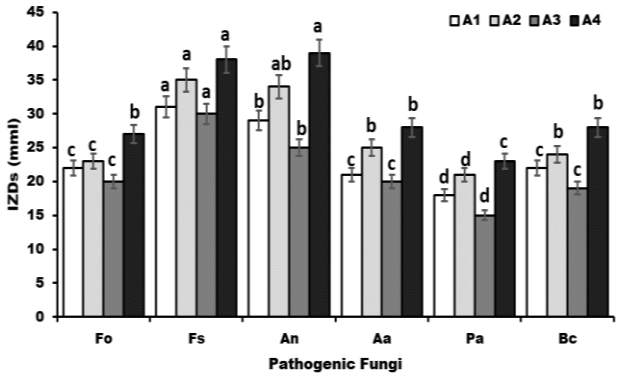

Fig. 7: Antifungal activity of SME against pathogenic fungi *Fusarium oxysporum (Fo), F. solani (Fs), Aspergillus niger (An), Alternaria alternata (Aa), Pythium aphanidermatum (Pa)*, and *Botrytis cinerea (Bc)*. Lowercase letters above columns indicate significant differences P<0.05.

Table 7: Assessment of the antimicrobial properties of SME

Samples	Concentration (µg/ml)	Inhibition Zone Diameter (mm)		
		Bacteria		Yeast
		B. cereus	*E. coli*	*C. albicans*
A1	100	9^{g}	8^{f}	10^{f}
	150	12^{f}	10^{e}	13^{e}
	200	18^{e}	15^{d}	17^{d}
A2	100	14^{f}	11^{e}	13^{e}
	150	17^{e}	14^{d}	17^{d}
	200	25^{c}	18^{c}	20^{c}
A3	100	17^{e}	15^{d}	16^{d}
	150	25^{c}	17^{c}	20^{c}
	200	29^{b}	23^{b}	25^{b}
A4	100	21^{d}	17^{c}	19^{c}
	150	28^{b}	21^{bc}	23^{bc}
	200	33^{a}	26^{a}	28^{a}

A1: callus derived from the root explants on M medium. A2: callus derived from the root explants on M3 medium. A3: callus derived from the root explants on M4 medium. A4: callus derived from the root explants on M10 medium. Lowercase letters in each column significantly indicated the differences between treatments.

In Vivo Experiment

Hepatoprotective Effect: Table 9 illustrates that the SME (M10 medium: MeJA treatment at 100 µM) provided liver protection, evidenced by significant downregulation of liver enzymes (AST, ALT, and ALP) in the SME-treated group relative to the $HgCl_2$ group. Incorporating SME into the rats' diets improved liver enzyme levels (75, 32, and 189 IU/L), representing a relative decrease of 25-35% compared to the control and a 2.9-3.8-fold decrease compared to the $HgCl_2$ group. Conversely, protein, albumin, and globulin levels increased in the SME-treated group (T2), while their levels also improved in T3. SME 200 was the optimal dose, delivering the best results across most parameters. There is a significant decrease in AST, ALT, ALP, and glucose, accompanied by an increase in total protein, albumin, and globulin, indicating an overall improvement in liver health, immunity, and glucose regulation.

Neuroprotective activity (Anti-Alzheimer): This study investigated the ability of SME to inhibit acetylcholinesterase (AChE), an enzyme linked to Alzheimer's disease. The study compared the inhibitory effects of these SME to those of donepezil, a commonly used AChE inhibitor medication. Results demonstrated that the SME at a concentration of 200 µg/mL exhibited the most potent AChE inhibition, achieving an 86% reduction in enzyme activity, comparable to that of donepezil. The IC_{50} values (concentration required to inhibit 50% of enzyme activity) were 41.33 µg/mL for SME and 52.69 µg/mL for donepezil, as illustrated in Fig. 8.

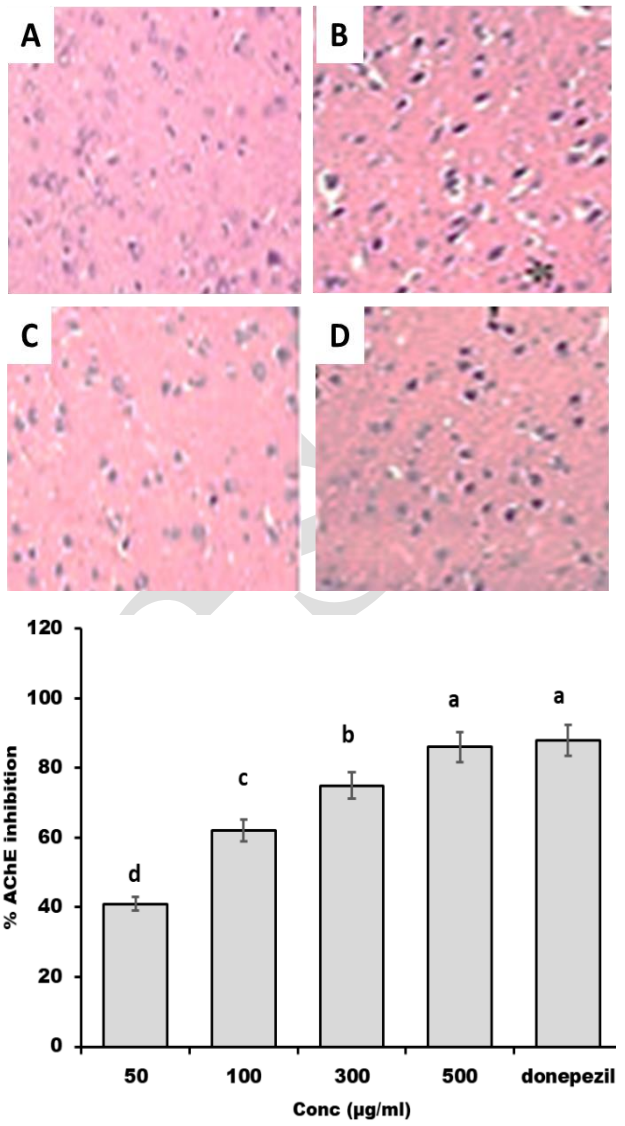

Fig. 8: A control rat brain showed normal tissues; B, Hg-challenged rats showed necrosis and gliosis in different regions of the hippocampus; C, SME-treated rats showed normal brain structure; D, recovered brain tissues after SME treatments; E, Anti-Alzheimer activity of SME compared to donepezil. Lowercase letters above each column indicate significant differences P<0.05.

SME extracts mitigated mercuric chloride ($HgCl_2$)-induced neuronal damage in the hippocampus. The $HgCl_2$ group exhibited significant necrosis (cell death) and gliosis (reactive glial response) in various hippocampal regions. In contrast, the control group and groups treated with 200 mg/kg of SME showed no necrosis or gliosis. In the $HgCl_2$ + SME 200 group, the severity of necrosis and gliosis was markedly reduced compared to the $HgCl_2$ group alone.

Intestinal gut microbiota: Table 10 presents data on microbial populations in the rats' gastrointestinal tracts. The control group displayed the highest counts of total bacteria, yeasts, molds, and *E. coli* (7.2, 3.9, and 5.7 Log_{10}

Table 8: Comprehensive evaluation of Milk Thistle Extract (SME) cytotoxicity and antiviral efficacy against Human Parvovirus B19 (PVB-19) and Sapporo Virus (SaV)

Parameter	Experimental Details	PVB-19 Results	SaV Results	Interpretation
Cytotoxicity (CC_{50}) (µg/mL)	MTS assay in Vero/BHK21 cells after 48h exposure (0-200 µg/mL range)	>150 (both cell lines)	>150 (both cell lines)	Low cytotoxicity enables safe therapeutic application
Antiviral IC_{50} (µg/mL)	CPE reduction assay (MOI=1, 48hpi) with SME (10-100 µg/mL)	32.1±1.8 µg/mL	44.9±2.3	PVB-19 shows greater sensitivity to SME treatment
Maximum Inhibition	Percentage CPE reduction at 100 µg/mL SME (vs. virus control)	89.2±3.1%[a]	76.4±2.7%[b]	Near-complete inhibition of PVB-19 at the highest dose
Selectivity Index (SI)	CC_{50}/IC_{50} ratio	4.68[a]	3.34[b]	PVB-19 has a superior therapeutic window
Cell Viability Rescue	MTS viability in infected cells treated with 100 µg/mL SME (vs. untreated infected)	82.3±4.2%[a]	70.8±3.9%[b]	SME restores metabolic activity in infected cells
Dose-Response Correlation	R^2 value from inhibition curves (10-100 µg/mL)	0.983	0.961	Strong concentration-dependent effects for both viruses

Lowercase letters in each raw significantly indicated the differences between treatments

CFU/g, respectively). A diet containing different concentrations of silymarin extracted from the medium (M10 medium: MeJA treatment at 100 µM) resulted in a 30-40% reduction in these harmful microorganisms among the rat groups. Lactic acid bacteria showed the lowest count in the control group (3.2 Log_{10} CFU/g), while their numbers increased upon SME incorporation into the diet,peaking at the highest SME levels (4.8 Log_{10} CFU/g). SME 500 provided the best overall results, showing a strong antimicrobial effect against harmful bacteria (total bacteria and *E. coli*) and molds/yeasts while promoting the growth of beneficial lactic acid bacteria.

Table 9: The hepatoprotective effects of an SME extract produced in M10 medium on $HgCl_2$-challenged rats.

Parameters	Control	$HgCl_2$	SME 200	$HgCl_2$+SME
AST (IU/L)	95[b]	285[a]	75[d]	85[c]
ALT(IU/L)	45[b]	120[a]	32[c]	40[b]
ALP(IU/L)	260[b]	533[a]	189[c]	210[bc]
Glucose (mg/dl)	141[a]	139[ab]	100[c]	128[b]
Total protein (g/dl)	8.1[b]	6.2[c]	9.5[a]	8.5[b]
Albumin (g/dl)	5.1[b]	4.0[c]	6.2[a]	5.8[ab]
Globulin (g/dl)	3.3[b]	2.3[c]	4.5[a]	4.0[ab]

Alanine transaminase (ALT), aspartate transaminase (AST), and alkaline phosphatase (ALP) Lowercase letters in each row significantly indicated the differences between treatments

Table 10: Effect of dietary treatments of an SME extract produced on M10 medium on the intestinal microbial count in rats.

Microbial count	Control	$HgCl_2$	SME 200	$HgCl_2$+SME
Total bacterial count	7.2[a]	7.5[a]	5.0[b]	5.7[b]
Total molds and yeasts	3.9[ab]	4.3[a]	2.5[b]	2.9[b]
Escherichia coli	5.7[b]	6.2[a]	3.2[d]	4.3[c]
Lactic acid bacteria	3.2[b]	1.9[c]	4.8[a]	4.2[ab]

Lowercase letters in each row significantly indicated the differences between treatments

Relative gene expression of proinflammatory and precancerous markers: The results in Fig. 9 strongly suggest that exposure to mercury chloride ($HgCl_2$) induces significant inflammation, with approximately a 600% increase in IL-1β (Fig. 9A) and an 800% increase in TNF-α (Fig. 9B) relative to the control group. Furthermore, $HgCl_2$ exposure leads to a substantial increase in apoptosis, as indicated by a roughly 550% increase in BAX (Fig. 9C) and a 450% increase in Casp-3 (Fig. 9D) expression compared to the control.

The administration of silymarin (200 mg/kg) along with mercury chloride (T3 group) demonstrates a protective effect. Silymarin treatment resulted in an approximate 60% reduction in IL-1β (Fig. 9A), a 65% reduction in TNF-α (Fig. 9B), a 50% reduction in BAX (Fig. 9C), and a 55% reduction in Casp-3 (Fig. 9D) relative expression compared to the $HgCl_2$-challenged group (G2). However, it's essential to note that silymarin did not eliminate the effects of mercury chloride, as the levels of these markers in the G3 group remained elevated compared to the control group (G1). Specifically, IL-1β was still approximately 200% higher, TNF-α roughly 250% higher, BAX about 150% higher, and Casp-3 around 100% higher in the T3 group compared to the control.

Histopathology: Fig. 10 displays histological sections of the liver and intestines from Wistar rats subjected to varying levels of SME (100, 300, and 500 mg/kg diet) extracts from (M10 medium: MeJA treatment at 100 µM). Microscopic examinations of liver sections revealed the normal appearance of the hepatic central vein and cords within the control group, with normal histological structures in the SME 200 mg/kg group. The $HgCl_2$-challenged group (G2) demonstrably exhibits significant hepatocellular damage. This is evidenced by widespread cellular swelling (ballooning degeneration), where the hepatocytes appear enlarged and pale. Clear signs of necrosis are present, with some cells displaying condensed or fragmented nuclei (pyknosis and karyorrhexis), as indicated by the darker, smaller nuclei pointed out by some arrows.

Furthermore, the normally organized cord-like arrangement of hepatocytes is disrupted. In contrast, the Silymarin + $HgCl_2$ group (G4) shows a notable reduction in the severity of this damage. The hepatocytes appear more normal in size and staining, with fewer instances of necrosis. The liver tissue architecture is better maintained, confidently indicating that silymarin provides a protective effect against the hepatotoxic effects of mercury chloride. Intestinal sections from the control group showed normal villi and mucosal architecture, while those from the group receiving the SME 200 mg/kg diet displayed regular intestinal features. The $HgCl_2$-challenged group (G2) displays significant damage to the intestinal villi. This includes a clear blunting and shortening of the villi, as highlighted by the arrows pointing to less elongated structures. The epithelial lining is disrupted, with evidence of cellular damage. In stark contrast, the Silymarin + $HgCl_2$ group (G4) shows a marked improvement in the preservation of the intestinal villi. The villi are longer and slimmer, with a more intact epithelial lining, confidently demonstrating silymarin's protective action against mercury chloride-induced intestinal damage.

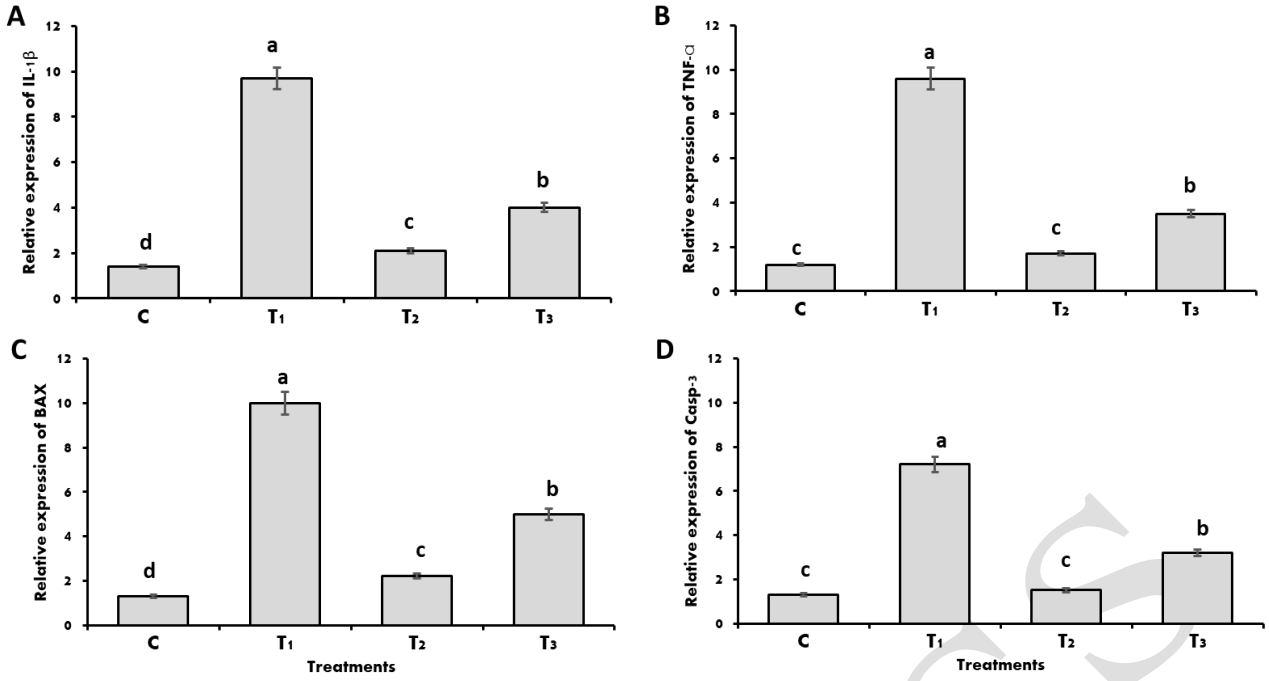

Fig. 9: The effect of SME on proinflammatory cytokines, and precancerous markers in $HgCl_2$-stressed rats. C (Control group receiving a basal diet), T1 $HgCl_2$-challenged rats, T2 (Silymarin 200 mg/kg), and T3 (Silymarin 200 mg/kg+$HgCl_2$). Lowercase letters above columns indicate significant differences $P<0.05$.

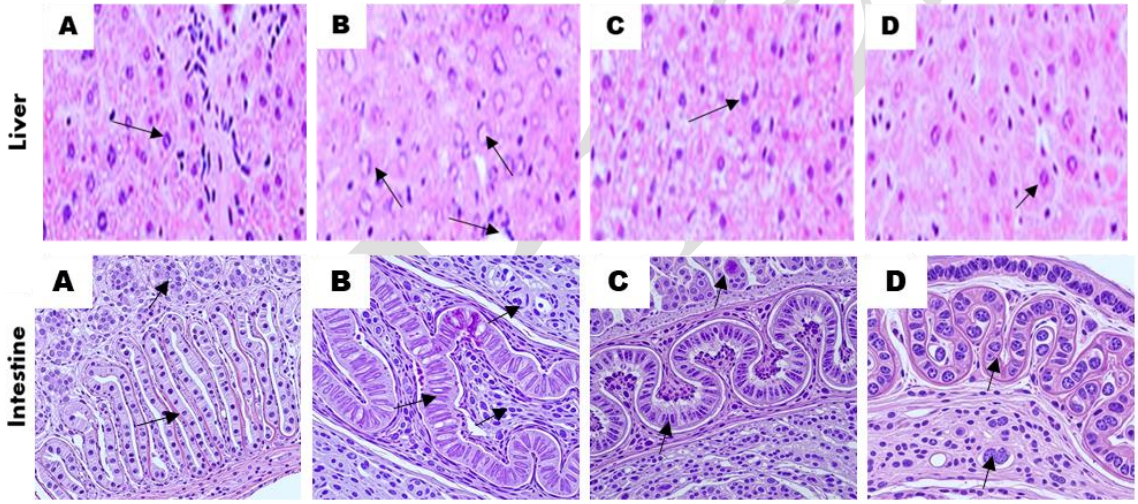

Fig. 10: visually compares liver and intestinal tissue from rats treated with silymarin (200 mg/kg). A (Control group receiving a basal diet), B $HgCl_2$-challenged rats, C (Silymarin 200 mg/kg), and D (Silymarin 200 mg/kg+$HgCl_2$). Each figure displays liver tissue (top row) and intestinal tissue (bottom row), stained with Hematoxylin and Eosin (H&E) to visualize tissue structure.

DISCUSSION

This study examined the influence of plant growth regulators (PGRs), explant type, and elicitors on callus formation, biomass yield, silymarin production, and various biological activities in *Silybum marianum* L. The role of PGRs was found to be crucial for initiating callus development in *S. marianum* tissues, as no callus formed in the control medium lacking PGRs, underscoring their importance (Khan *et al.,* 2018; Saleem *et al.,* 2022). The research evaluated different combinations and concentrations of two specific PGRs: 2,4-D and kinetin (Kin). Results revealed a notable interaction between these regulators and explant type. Callus formation did not occur with either 2,4-D or Kin alone; however, their combination induced callus formation after 60 days of culture. Auxins such as 2,4-D promote dedifferentiation in explant cells, while the combination of auxin and cytokinin facilitates rapid callus growth and formation (Kaur *et al.,* 2018; Mayerni *et al.,* 2020).

Previous studies have reported the presence of cytoplasmic parenchymatous cells in the callus of *Bacopa racemosa* (Dalila *et al.,* 2013) and *Arabidopsis thaliana* (Li *et al.,* 2017) when using a combination of kinetin and 2,4-D, suggesting an enhancement of the cytoplasm in parenchyma cells. However, kinetin alone did not stimulate this cytoplasmic development and was associated with significant vacuolation, as noted by Mastuti *et al.* (2017). Meanwhile, 2,4-D is necessary for callus induction, while kinetin aids in its proliferation. Thus,

auxins primarily drive callus formation, whereas kinetin promotes its growth and multiplication, indicating a synergistic effect that activates the developmental pathways necessary for callus initiation (Saleem *et al.,* 2022).

The optimal concentrations of 2,4-D and Kin for callus induction varied depending on explant type (root, hypocotyl, or leaf). Notably, root explants generally showed stronger callus induction with higher concentrations of both PGRs, suggesting a more robust response compared to leaf or hypocotyl explants, which required lower PGR concentrations for optimal callus formation (Bolouri *et al.,* 2019). In contrast, some studies reported higher callus induction frequencies in epicotyl and leaf explants than in root explants (Cardi and Monti, 1990; Sidhu *et al.,* 2023). The interaction between PGR concentration and explant type was statistically significant (Ewes *et al.,* 2023; Marković *et al.*, 2023), highlighting the need to consider both factors when developing protocols for callus induction in *S. marianum* L.

In the second phase of the study, the effects of elicitors on callus growth and silymarin production were examined. Two elicitors—methyl jasmonate (100 µM) and yeast extract (4 mg/L) were used. Both significantly ($P<0.05$) enhanced callus growth, as measured by cell dry weight. Specifically, methyl jasmonate treatment resulted in a 2.59-fold increase in cell dry weight compared to the control, with yeast extract producing a similar effect (Demidova *et al.,* 2023; Khadem, 2023). The study also explored how varying concentrations of PGRs and elicitors during cell culture affected total phenolic content (TPC). PGRs influence plant growth and development, while elicitors can stimulate the production of specific metabolites, including phenolics. A significant variance in TPC among the extracts indicated that treatments with PGRs and elicitors substantially affected phenolic production. The focus was placed on extracts with the highest phenolic content, as these are most promising for further investigation due to their likely enhanced biological activities.

In recent years, growing awareness of the importance of a nutritious diet for maintaining overall health has highlighted the significance of plant-derived bioactive compounds, which have attracted considerable attention for their functional properties and potential to prevent various diseases (Reda *et al.,* 2024b; El-Saadony *et al.,* 2025a,b). Phenolic compounds are secondary metabolites of plants, which are recognized for their antioxidant properties and associated health benefits (Saad *et al.,* 2021; Mueed *et al.,* 2024). The free radical scavenging ability of the extracts was evaluated, revealing that all tested extracts exhibited potent antioxidant activity (Selim *et al.,* 2022; Alharbi *et al.,* 2024). Notably, extracts from callus cultures treated with elicitors demonstrated even greater antioxidant effects than those treated with PGRs alone, suggesting that elicitors may further boost the plant's defense mechanisms. Additionally, the extracts showed notable antimicrobial activity against *Bacillus subtilis*, highlighting their potential as natural antimicrobial agents, although pathogens such as *Candida albicans* and *Escherichia coli* exhibited greater resistance. Remarkably, silymarin-rich extracts displayed a strong capacity to inhibit the proliferation of human liver cancer cells, with effects comparable to doxorubicin (DOX), a well-known anticancer drug.

Microscopic observations supported these findings, indicating a direct effect of the extracts on cancer cell health. A clear relationship was observed between extract concentration and anticancer effectiveness, with higher concentrations (lower IC_{50} values) producing more significant inhibition. Previous research has shown that silymarin can regulate hepatic fatty acid beta-oxidation, influence bile acid metabolism, and modulate intestinal glucose metabolism via the peroxisome proliferator-activated receptor pathway, functions that are vital for maintaining lipid homeostasis in the liver and intestines (Zakaria *et al.,* 2023).

Furthermore, the combined effect of enhanced hepatic antioxidant compound activity and increased hepatic glycogen levels in response to silymarin treatment suggests its potential as a supplementary therapy for chronic liver conditions such as hepatitis, tissue damage, and steatohepatitis. Swedish *Silybum marianum* fruit extracts (FSE) have been shown to significantly reduce hepatic fat deposition as well as serum cholesterol and triglyceride levels in rats with high-fat diet-induced obesity. Additionally, Kim et al. reported that silymarin may aid in recovery from inflammation and fatigue in rats subjected to high-intensity training (Ezhilarasan *et al.,* 2022; Yang et al., 2022; Zakaria et al., 2023).

The primary active compound in silymarin is silybin (or silibin), which consists of two isomers: silybin A and silybin B, the main effective constituents. Other flavonoids, including isosilybin A, isosilybin B, silychristin, and silydianin, are also present. Both in vitro and clinical research indicate that silymarin possesses substantial anti-inflammatory, antifibrotic, antioxidant, and cytoprotective properties. These effects suggest that silymarin may be a viable option for chronic liver diseases. Importantly, the diverse effects of silymarin may not be solely due to its antioxidant properties; other mechanisms, such as protection of mitochondrial function, regulation of retinoic acid metabolism, cell cycle arrest, induction of apoptosis, and chemoresistance to erythromycin, may also be involved. The present study demonstrated significant effects of silymarin in lowering serum transaminase levels, enhancing hepatic and intestinal antioxidant compounds, and regulating fatty acid beta-oxidation, bile acid metabolism, and glucose metabolism in both the liver and intestine (Petrásková *et al.,* 2020; Vecera *et al.,* 2022; Mihailović et al., 2023; Al Hashmi *et al.,* 2024).

Improvement in gut integrity was observed, preventing the translocation of hepatotoxic metabolites and bacterial endotoxins to the liver via the portal circulation (Plaza-Díaz *et al.,* 2020). These microbiota-mediated effects create a protective cascade: reduced LPS levels suppress TLR4/NF-κB signaling pathways, thereby decreasing hepatic inflammation (Xiao *et al.,* 2024); meanwhile, increased SCFA production contributes to antioxidant defenses and metabolic regulation. Furthermore, silymarin's modulation of gut microbial communities enhances liver detoxification by upregulating phase II enzymes (Jin *et al.,* 2024). By restoring gut microbial balance and reinforcing the gut-liver axis, silymarin shows therapeutic potential for various liver conditions, including non-alcoholic fatty liver disease (NAFLD), cirrhosis, and drug-induced hepatotoxicity (Wang *et al.,* 2024).

A general decrease in the Bacteroidetes and Actinobacteria phyla was observed among gut bacteria in the silymarin treatment groups, while the Proteobacteria phylum increased. In contrast, chemical medication decreased all counts (Pandey *et al.,* 2023). Through its antimicrobial properties, silymarin preferentially inhibits pathogenic bacteria, such as *Escherichia coli* and *Clostridium* species, while preserving beneficial commensal microbiota, including *Lactobacillus* and *Bifidobacterium* (Zarenezhad *et al.,* 2023). This selective inhibition helps maintain microbial equilibrium, reducing gut dysbiosis and the production of harmful endotoxins such as lipopolysaccharides (LPS) (Candelli et al., 2020).

Positive and negative correlations existed among the bacterial groups. Principal coordinates analysis clearly distinguished the five rat groups, and no pathogenic bacterial groups were found in the feces, indicating that administration of 5 g of silymarin as an antioxidant posed no toxic effects. As an antioxidative compound, silymarin primarily protects the liver from damage. Compounds with liver-protective effects may also influence gut microbiota composition, subsequently impacting liver health. To analyze shifts in gut bacteria after silymarin treatment, DNA was isolated from rat feces, revealing 84 different gut bacterial species across the five groups. Five bacterial phyla were identified: Bacteroidetes, Firmicutes, Proteobacteria, Actinobacteria, and Verrucomicrobia (Li *et al.,* 2020; Xu *et al.,* 2022; Wang *et al.,* 2024).

Conclusions: This study demonstrated that methyl jasmonate (MeJA) significantly enhances silymarin production in *Silybum marianum* L. cell suspension cultures, yielding a potent extract rich in silymarin components. The resulting MeJA-silymarin-enriched extract (SME) exhibited multiple beneficial activities, including antiviral, antidiabetic, antimicrobial, anticancer, and neuroprotective effects. Notably, in $HgCl_2$-challenged rats, SME effectively mitigated liver damage by downregulating proinflammatory genes, reducing liver enzyme and glucose levels, and preserving the integrity of both liver and intestinal tissues. Furthermore, SME promoted a beneficial gut microbial profile and demonstrated significant acetylcholinesterase inhibition, suggesting its potential to prevent neurodegeneration. Collectively, these findings establish MeJA as a promising elicitor for maximizing silymarin production and underscore the therapeutic potential of SME as a natural hepatoprotective and gut-regulatory agent against oxidative stress-induced damage. Future research should focus on isolating specific bioactive components and conducting clinical trials to validate these preclinical findings and further explore the full therapeutic potential of silymarin-enriched extracts.

Competing interests: The authors declare that they have no competing interests.

Author Contributions: Conceptualization, AAA, NBI, SSS, TAI, and AAH, formal analysis, JAA, ANA, KAM, AOS, AA, EAB, HK AG, MAA, AEA, and MAK, investigation, AAA, NBI, ANA, SSS, TAI, and AAH, data curation, JAA, KAM, AOS, AA, EAB, HK AG, MAA, AEA, and MAK, writing original draft preparation, AAA, NBI, SSS, ANA,TAI, and AAH, writing final manuscript and editing, JAA, KAM, AOS, AA, EAB, HK AG, MAA, AEA, and MAK, visualization and methodology, AAA, NBI, SSS, TAI, ANA, JAA, KAM, AOS, AA, EAB, HK AG, MAA, AEA, ANA, MAK, and AAH. All authors have read and agreed to the published version of the manuscript.

Acknowledgments: The project was funded by KAU Endowment (WAQF) at king Abdulaziz University, Jeddah, Saudi Arabia. The authors, therefore, acknowledge with thanks WAQF and the Deanship of Scientific Research (DSR) for technical and financial support. The authors gratefully acknowledge Princess Nourah bint Abdulrahman University Researchers Supporting Project number (PNURSP2025R892), Princess Nourah bint Abdulrahman University, Riyadh, Saudi Arabia. The authors extend their appreciation to the deanship of scientific research at King Khalid University for supporting this work under the large research group number (R.G.P2/330/46).

Funding: The project was funded by KAU Endowment (WAQF) at king Abdulaziz University, Jeddah, Saudi Arabia. The authors, therefore, acknowledge with thanks WAQF and the Deanship of Scientific Research (DSR) for technical and financial support. This research was funded by Princess Nourah bint Abdulrahman University Researchers Supporting Project number (PNURSP2025R892), Princess Nourah bint Abdulrahman University, Riyadh, Saudi Arabia, and King Khalid University for supporting this work under the large research group number (R.G.P2/330/46).

REFERENCES

Abd El-Wahab AEWAEA, Aly MMM, Bahnas MS, *et al.,* 2022. Influence of dietary supplementation of marigold flower powder and extract (*Calendula officinalis* L.) on performance, nutrient digestibility, serum biochemistry, antioxidant parameters and immune responses of growing Japanese quail. J Anim Physiol Anim Nutr 106:742-751. DOI: 10.1111/jpn.13611

Abdel-Moneim A-ME, El-Saadony MT, Shehata AM, *et al.,* 2022. Antioxidant and antimicrobial activities of Spirulina platensis extracts and biogenic selenium nanoparticles against selected pathogenic bacteria and fungi. Saudi J Biol Sci 29:1197-1209. https://doi.org/10.1016/j.sjbs.2021.09.046

Abdul Malik NA, Kumar IS, Nadarajah K, 2020. Elicitor and receptor molecules: orchestrators of plant defense and immunity 21(3):963. doi: 10.3390/ijms21030963

Ahmad I, Basra SMA, Akram M, *et al.,* 2017. Improvement of antioxidant activities and yield of spring maize through seed priming and foliar application of plant growth regulators under heat stress conditions. Semina Ciênc Agrár 38:47-56. DOI: 10.5433/1679-0359.2017v38n1p47

Al Hashmi K, Giglio RV, Pantea Stoian A, *et al.,* 2024. Metabolic dysfunction-associated fatty liver disease: current therapeutic strategies. Front Nutr 11:1355732. doi: 10.3389/fnut.2024.1355732

Albassam AA, Frye RF, Markowitz JS, 2017. The effect of milk thistle (*Silybum marianum*) and its main flavonolignans on CYP2C8 enzyme activity in human liver microsomes. Chem Biol Interact 271:24-29. https://doi.org/10.1016/j.cbi.2017.04.025

Alharbi YM, Elzahar KM, Qahl SH, *et al.,* 2024. Nutritional significance, antimicrobial, antioxidants, anticancer, and antiviral activities of lemongrass leaves extract and its application as hepatoprotective agent against CCl_4-Induced hepatic injury in rats. An Acad Bras Ciênc 96(3): e20230646. https://doi.org/10.1590/0001-3765202420230646

Ali M, Abbasi BH, Ali GS, 2015. Elicitation of antioxidant secondary metabolites with jasmonates and gibberellic acid in cell suspension cultures of *Artemisia absinthium* L. Plant Cell, Tissue And Organ Culture (PCTOC) 120, 1099-1106. https://doi.org/10.1007/s11240-014-0666-2

Al-Quwaie DA, Allohibi A, Aljadani M, *et al.,* 2023. Characterization of Portulaca oleracea whole plant: Evaluating antioxidant, anticancer, antibacterial, and antiviral activities and application as quality enhancer in yogurt. Molecules 28(15):5859. https://doi.org/10.3390/molecules28155859

Alshehri FS, Kotb E, Nawaz M, *et al.,* 2022. Preparation, characterization, and antibacterial competence of silymarin and its nano-formulation. J Exp Nanosci 17:100-112. https://doi.org/10.1080/17458080.2022.2041192

Alsubhi NH, Al-Quwaie DA, Alrefaei GI, *et al.,* 2022. Pomegranate pomace extract with antioxidant, anticancer, antimicrobial, and antiviral activity enhances the quality of strawberry-yogurt smoothie. Bioengineering 9(12): 735. https://doi.org/10.3390/bioengineering9120735

Baenas N, García-Viguera C, Moreno DA, 2014. Elicitation: a tool for enriching the bioactive composition of foods. Molecules 19(9):13541–13563. doi: 10.3390/molecules190913541

Bekheet S, 2011. *In vitro* biomass production of liver-protective compounds from Globe artichoke (*Cynara scolymus* L.) and Milk thistle (*Silybum marianum*) plants. Emir J Food Agric 23(5):473-481

Bolouri P, Pour AH, Jannati G, *et al.,* 2019. Genetic diversity of Pea (*Pisum arvense* L.) genotypes according to the tissue culture traits. Atatürk. Üniv. Ziraat. Fak. Derg 50:11-17. https://doi.org/10.17097/ataunizfd.413006

Cacho M, Morán M, Corchete P, *et al.,* 1999. Influence of medium composition on the accumulation of flavonolignans in cultured cells of *Silybum marianum* (L.) Gaertn. Plant Sci 144:63-68. https://doi.org/10.1016/S0168-9452(99)00056-4

Cadamuro J, Mrazek C, Leichtle B, *et al.,* 2018. Influence of centrifugation conditions on the results of 77 routine clinical chemistry analytes using standard vacuum blood collection tubes and the new BD-Barricor tubes. Biochemia Medica 28(1): 55-64. doi: 10.11613/BM.2018.010704

Candelli M, Franza L, Pignataro G, *et al.,* 2021. Interaction between lipopolysaccharide and gut microbiota in inflammatory bowel diseases. Int J Mol Sci 22(12): 6242. DOI: 10.3390/ijms22126242

Cardi T, Monti L, 1990. Optimization of callus culture in pea (*Pisum sativum* L.). Annali della Facoltà di Scienze Agrarie della Università degli Studi di Napoli, Portici 24:11-18.

Dalila ZD, Jaafar H, Manaf AA, 2013. Effects of 2, 4-D and kinetin on callus induction of Barringtonia racemosa leaf and endosperm explants in different types of basal media. Asian J Plant Sci 12:21-27. DOI: 10.3923/ajps.2013.21.27

Demidova E, Globa E, Klushin A, *et al.,* 2023. Effect of methyl jasmonate on the growth and biosynthesis of $C1_3$- and $C1_4$-Hydroxylated taxoids in the cell culture of yew (*Taxus wallichiana* Zucc.) of different ages. Biomolecules 13(6): 969. https://doi.org/10.3390/biom13060969

Dong S, Nie H, Ye J, *et al.,* 2020. Physiological and gene expression analysis of the Manila clam Ruditapes philippinarum in response to cold acclimation. Sci Total Environ 742: 140427. https://doi.org/10.1016/j.scitotenv.2020.140427

El-Hawwary SS, Abd Almaksoud HM, Saber FR, *et al.,* 2021. Green-synthesized zinc oxide nanoparticles, anti-Alzheimer potential and the metabolic profiling of Sabal blackburniana grown in Egypt supported by molecular modelling. RSC Adv 11:18009-18025. https://doi.org/10.1039/D1RA01725J

El-Saadony MT, Saad AM, Korma SA, *et al.,* 2024a. Garlic bioactive substances and their therapeutic applications for improving human health: A comprehensive review. Front Immunol 15:1277074. https://doi.org/10.3389/fimmu.2024.1277074

El-Saadony MT, Yang T, Saad AM, *et al.,* 2024b. Polyphenols: Chemistry, bioavailability, bioactivity, nutritional aspects and human health benefits: A review. Int J Biol Macromol 27(3): 134223. https://doi.org/10.1016/j.ijbiomac.2024.134223

El-Saadony MT, Saad AM, Alkafaas SS, *et al.,* 2025a. Chitosan, derivatives, and its nanoparticles: Preparation, physicochemical properties, biological activities, and biomedical applications–A comprehensive review. Int J Biol Macromol 313: 142832. https://doi.org/10.1016/j.ijbiomac.2025.142832

El-Saadony MT, Saad AM, Mohammed DM, *et al.,* 2025b. Medicinal plants: bioactive compounds, biological activities, combating multidrug-resistant microorganisms, and human health benefits-a comprehensive review. Front Immunol 16: 1491777. https://doi.org/10.3389/fimmu.2025.1491777

El-Saadony MT, Yang T, Korma SA, *et al.,* 2023b. Impacts of turmeric and its principal bioactive curcumin on human health: Pharmaceutical, medicinal, and food applications: A comprehensive review. Front Nutr 9: 1040259. https://doi.org/10.3389/fnut.2022.1040259

El-Saadony MT, Zabermawi NM, Zabermawi NM, *et al.,* 2023a. Nutritional aspects and health benefits of bioactive plant compounds against infectious diseases: a review. Food Rev Int 39(4): 2138-2160. https://doi.org/10.1080/87559129.2021.1944183

El-Sapagh S, Allam NG, El-Sayed MNE-D, *et al.,* 2023. Effects of *Silybum marianum* L. seed extracts on multi drug resistant (MDR) bacteria. Molecules 29(1): 64. https://doi.org/10.3390/molecules29010064

Elsawy H, Alzahrani AM, Alfwuaires M, *et al.,* 2021. Analysis of silymarin-modulating effects against acrylamide-induced cerebellar damage in male rats: biochemical and pathological markers. J Chem Neuroanat 115:101964. https://doi.org/10.1016/j.jchemneu.2021.101964

Elwekeel A, AbouZid S, Sokkar N, *et al.,* 2012. Studies on flavanolignans from cultured cells of *Silybum marianum*. Acta Physiol Plant 34:1445-1449. https://doi.org/10.1007/s11738-012-0942-x

Ewes H, Abdel-Raheem A, Salha A, *et al.,* 2023. Effect of different concentrations and combinations of some plant growth regulators on *Punica granatum* anther culture. Curr Chem Lett 12:257-264. DOI: 10.5267/j.ccl.2023.1.003

Ezhilarasan D, Lakshmi T, 2022. A molecular insight into the role of antioxidants in nonalcoholic fatty liver diseases. Oxid Med Cell Longev 2022:9233650. DOI: 10.1155/2022/9233650

Ghodousi M, Karbasforooshan H, Arabi L, *et al.,* 2023. Silymarin as a preventive or therapeutic measure for chemotherapy and radiotherapy-induced adverse reactions: a comprehensive review of preclinical and clinical data. Eur J Clin Pharmacol 79:15-38. DOI: 10.1007/s00228-022-03434-8

Goyal S, Lambert C, Cluzet S, *et al.,* 2012. Secondary metabolites and plant defence. Plant defence: Biocontrol 109-138. https://doi.org/10.1007/978-94-007-1933-0_5

Graf TN, Wani MC, Agarwal R, *et al.,* 2007. Gram-scale purification of flavonolignan diastereoisomers from *Silybum marianum* (Milk Thistle) extract in support of preclinical in vivo studies for prostate cancer chemoprevention. Planta Med 73:1495-1501. DOI: 10.1055/s-2007-990239

Hall CR, Mikhael M, Hartley SE, *et al.,* 2020. Elevated atmospheric CO_2 suppresses jasmonate and silicon-based defences without affecting herbivores. Funct Ecol 34:993-1002. https://doi.org/10.1111/1365-2435.13549

He M, He C-Q, Ding N-Z, 2018. Abiotic stresses: general defenses of land plants and chances for engineering multistress tolerance. Front Plant Sci 9:1771. https://doi.org/10.3389/fpls.2018.01771

Isah T, Umar S, Mujib A, *et al.,* 2018. Secondary metabolism of pharmaceuticals in the plant in vitro cultures: strategies, approaches, and limitations to achieving higher yield. Plant Cell, Tissue and Organ Culture 132:239-265. https://doi.org/10.1007/s11240-017-1332-2

Jin Y, Wang X, Chen K, *et al.,* 2024. Silymarin decreases liver stiffness associated with gut microbiota in patients with metabolic dysfunction-associated steatotic liver disease: a randomized, double-blind, placebo-controlled trial. Lipids Health Dis 23(1): 239. DOI: 10.1186/s12944-024-02220-y

Kaur A, Malhotra PK, Manchanda P, *et al.,* 2018. Micropropagation and Somatic Embryogenesis in Sugarcane. In: Gosal SS, Wani SH, editors. Biotechnologies of Crop Improvement, Volume 1: Cellular Approaches. Cham: Springer International Publishing p 57-91. DOI https://doi.org/10.1007/978-3-319-78283-6

Khadem A, 2023. Cell suspension culture of lavender (*Lavandula angustifolia*) and the influence of methyl jasmonate and yeast extract on rosmarinic acid production. J Med Plants 22(87): 114-130. 10.61186/jmp.22.87.114

Khan T, Abbasi BH, Khan MA, 2018. The interplay between light, plant growth regulators and elicitors on growth and secondary metabolism in cell cultures of *Fagonia indica*. J Photochem Photobiol B: Biol 185:153-160. https://doi.org/10.1016/j.jphotobiol.2018.06.002

Khojali WM, Hussein W, Bin Break MK, *et al*., 2023. Chemical composition, antibacterial activity and in vitro anticancer evaluation of *Ochradenus baccatus* methanolic extract. Medicina 59(3): 546. https://doi.org/10.3390/medicina59030546

Lani R, Hassandarvish P, Chiam CW, *et al.,* 2015. Antiviral activity of silymarin against chikungunya virus. Sci Rep 5(1): 11421. https://doi.org/10.1038/srep11421

Li S, Huang P, Ding G, *et al.,* 2017. Optimization of hormone combinations for root growth and bud germination in Chinese fir (*Cunninghamia*

lanceolata) clone leaf cuttings. Sci Rep 7:5046. DOI https://doi.org/10.1038/s41598-017-05295-z

Li X, Wang Y, Xing Y, *et al.,* 2020. Changes of gut microbiota during silybin-mediated treatment of high-fat diet-induced non-alcoholic fatty liver disease in mice. Hepatol Res 50:5-14. DOI: 10.1111/hepr.13444

Liang C, Chen C, Zhou P, *et al.,* 2018. Effect of *Aspergillus flavus* fungal elicitor on the production of terpenoid indole alkaloids in *Catharanthus roseus* cambial meristematic cells. Molecules 23:3276. https://doi.org/10.3390/molecules23123276

Livak KJ, and Schmittgen TD, 2001. Analysis of relative gene expression data using real-time quantitative PCR and the 2− ΔΔCT method. Methods 25(4): 402-408. https://doi.org/10.1006/meth.2001.1262

Low ZX, OuYong BM, Hassandarvish P, *et al.,* 2021. Antiviral activity of silymarin and baicalein against dengue virus. Sci Rep 11(1): 21221. DOI: 10.1038/s41598-021-98949-y

Makena W, Aribiyun YS, Aminu A, *et al.,* 2022. Flavonoids fractions of *Adansonia digitata* L. fruits protects adult Wistar rats from mercury chloride-induced hepatorenal toxicity: histopathological and biochemical studies. Egypt J Basic Appl Sci 9(1): 205-215. https://doi.org/10.1080/2314808X.2022.2059140

Marković M, Trifunović-Momčilov M, Radulović O *et al.,* 2023. The Effects of Different Auxin–Cytokinin Combinations on Morphogenesis of *Fritillaria meleagris* Using Bulb Scale Sections In Vitro. Horticulturae 9(8): 910. https://doi.org/10.3390/horticulturae9080910

Mastuti R, Munawarti A, Firdiana ER, 2017. The combination effect of auxin and cytokinin on in vitro callus formation of *Physalis angulata* L. – A medicinal plant. AIP Conf Proc 1908:040007. https://doi.org/10.1063/1.5012721

Mayerni R, Satria B, Wardhani DK, *et al.,* 2020. Effect of auxin (2, 4-D) and cytokinin (BAP) in callus induction of local patchouli plants (*Pogostemon cablin* Benth.). IOP Conf. Ser.: Earth Environ Sci 583 012003. DOI 10.1088/1755-1315/583/1/012003

Mihailović V, Srećković N, Popović-Djordjević JB, 2023. Silybin and Silymarin: Phytochemistry, bioactivity, and pharmacology. In: Handbook of dietary flavonoids: Springer 1-45. https://doi.org/10.1007/978-3-030-94753-8_20-1

Mosihuzzaman M, 2012. Herbal medicine in healthcare-an overview Nat Prod Commun 7(6):807-812. https://doi.org/10.1177/1934578X1200700628

Mueed A, Aljahdali SM, Albalawi M, *et al.,* 2024. Phenolic compounds and biological activities of berberis fruit: Enhancing role on physiochemical and antioxidant properties of yogurt. LWT-Food Sci Technol 211: 116834. https://doi.org/10.1016/j.lwt.2024.116834

Mueed A, Shibli S, Al-Quwaie DA, *et al.,* 2023. Extraction, characterization of polyphenols from certain medicinal plants and evaluation of their antioxidant, antitumor, antidiabetic, antimicrobial properties, and potential use in human nutrition. Front Nutr 10: 1125106. https://doi.org/10.3389/fnut.2023.1125106

Naik, P. M., Al-Khayri, J. M, 2016. Abiotic and biotic elicitors-role in secondary metabolites production through in vitro culture of medicinal plants. Abiotic and biotic stress in plants—recent advances and future perspectives. Rijeka: InTech 17: 247-77. DOI: 10.5772/61442

Nouri A, and Heidarian E, 2019. Nephroprotective effect of silymarin against diclofenac-induced renal damage and oxidative stress in male rats. J HerbMed Pharmacol 8(2): 146-152. **doi:** 10.15171/jhp.2019.23

Pandey B, Baral R, Kaundinnyayana A, *et al.,* 2023. Promising hepatoprotective agents from the natural sources: a study of scientific evidence. Egypt Liver J 13(1): 14. https://doi.org/10.1186/s43066-023-00248-w

Petrásková L, Káňová K, Biedermann D, *et al.,* 2020. Simple and rapid HPLC separation and quantification of flavonoid, flavonolignans, and 2, 3-dehydroflavonolignans in silymarin. Foods 9(2): 116; https://doi.org/10.3390/foods9020116

Plaza-Díaz J, Solís-Urra P, Rodríguez-Rodríguez F, *et al.,* 2020. The gut barrier, intestinal microbiota, and liver disease: molecular mechanisms and strategies to manage. Int J Mol Sci 21(21): 8351. DOI: 10.3390/ijms21218351

Reda FM, Alagawany M, Mahmoud HK, *et al.,* 2024b. Application of pumpkin oil as a new feed additive in Cobb Avian 48 broilers: its effect on performance, carcasses, digestive enzyme, blood metabolites and cecal bacterial load. J Appl Poult Res 33(4): 100480. https://doi.org/10.1016/j.japr.2024.100480

Reda FM, Alagawany M, Mahmoud HK, *et al.,* 2024a. Application of naringenin as a natural feed additive for improving quail performance and health. J Appl Poult Res 33(3):100446. https://doi.org/10.1016/j.japr.2024.100446

Ruiz-García Y, Gómez-Plaza E, 2013. Elicitors: A tool for improving fruit phenolic content. Agriculture 3(1): 33-52. https://doi.org/10.3390/agriculture3010033

Saad AM, Mohamed AS, El-Saadony MT, *et al.,* 2021. Palatable functional cucumber juices supplemented with polyphenols-rich herbal extracts. LWT-Food Sci Technol 148: 111668. https://doi.org/10.1016/j.lwt.2021.111668

Saeed M, Babazadeh D, Arif M, *et al.,* 2017. Silymarin: a potent hepatoprotective agent in poultry industry. World's Poult Sci J 73:483-492. https://doi.org/10.1017/S0043933917000538

Saleem Y, Emad MZ, Ali A, *et al.,* 2022. Synergetic Effect of Different Plant Growth Regulators on Micropropagation of Sugarcane (*Saccharum officinarum* L.) by Callogenesis. Agriculture 12:1812. https://doi.org/10.3390/agriculture12111812

Sánchez-Sampedro MA, Fernández-Tárrago J, Corchete P, 2005a. Yeast extract and methyl jasmonate-induced silymarin production in cell cultures of *Silybum marianum* (L.) Gaertn. J Biotechnol 119:60-69. https://doi.org/10.1016/j.jbiotec.2005.06.012

Sánchez-Sampedro MA, Fernández-Tárrago J, Corchete P, 2005b. Enhanced silymarin accumulation is related to calcium deprivation in cell suspension cultures of *Silybum marianum* (L.) Gaertn. J Plant Physiol 162:1177-1182. https://doi.org/10.1016/j.jplph.2005.01.012

Sánchez-Sampedro MA, Fernández-Tárrago J, Corchete P, 2008. Some common signal transduction events are not necessary for the elicitor-induced accumulation of silymarin in cell cultures of *Silybum marianum*. J Plant Physiol 165:1466-1473. https://doi.org/10.1016/j.jplph.2007.12.009

Selim S, Albqmi M, Al-Sanea MM, *et al.,* 2022. Valorizing the usage of olive leaves, bioactive compounds, biological activities, and food applications: A comprehensive review. Front Nutr 9:1008349. https://doi.org/10.3389/fnut.2022.1008349

Shah M, Nawaz S, Jan H, *et al.,* 2020. Synthesis of bio-mediated silver nanoparticles from Silybum marianum and their biological and clinical activities. Mater Sci Eng C 112:110889. https://doi.org/10.1016/j.msec.2020.110889

Sidhu G, Malhotra P, Rattanpal H, 2023. Optimization of explants, media, plant growth regulators and carbohydrates on callus induction and plant regeneration in Citrus jambhiri Lush. J Hortic Sci 18:162-172. DOI: https://doi.org/10.24154/jhs.v18i1.2159

Smetanska I, 2008. Production of secondary metabolites using plant cell cultures. Adv Biochem Eng Biotechnol 187-228. DOI: 10.1007/10_2008_103

Suvarna M, Niranjan U, 2013. Classification methods of skin burn images. Int J Inf Technol 5(1)109-118. DOI : 10.5121/ijcsit.2013.510

Vecera R, Poruba M, Hüttl M, *et al.,* 2022. Beneficial effect of fenofibrate and silymarin on hepatic steatosis and gene expression of lipogenic and cytochrome P450 enzymes in non-obese hereditary hypertriglyceridemic rats. Curr Issues Mol Biol 44:1889-1900. DOI: 10.3390/cimb44050129

Wang X, Jin Y, Di C, *et al.,* 2024. Supplementation of Silymarin alone or in combination with Salvianolic acids B and Puerarin regulates gut microbiota and its metabolism to improve high-fat diet-induced NAFLD in mice. Nutrients 16:1169. DOI: 10.3390/nu16081169

Wang X, Jin Y, Di C, *et al.,* 2024. Supplementation of silymarin alone or in combination with salvianolic acids B and puerarin regulates gut microbiota and its metabolism to improve high-fat diet-induced NAFLD in mice. Nutrients 16(8): 1169. https://doi.org/10.3390/nu16081169

Westgard JO, and Poquette MA, 1972. Determination of serum albumin with the" SMA 12/60" by a bromcresol green dye-binding method. Clinical Chem 18(7): 647–653. https://doi.org/10.1093/clinchem/18.7.647

Widholm J, 1972. The use of fluorescein diacetate and phenosafranine for determining viability of cultured plant cells. Stain Technol 47:189-194. DOI: 10.3109/10520297209116483

Xiao S, Li W, Zhang P, *et al.,* 2024. Mechanisms of food-derived bioactive compounds inhibiting TLR4 activation and regulating TLR4-mediated inflammation: A comprehensive review and future directions. Food Biosci 61:104587. https://doi.org/10.1016/j.fbio.2024.104587

Xu S, Jiang X, Jia X, *et al.,* 2022. Silymarin modulates microbiota in the gut to improve the health of sow from late gestation to lactation. Animals 12:2202. DOI: 10.3390/ani12172202

Yang B, Yang X, Tan X, *et al.,* 2022. Regulatory networks, management approaches, and emerging treatments of nonalcoholic fatty liver disease. Can J Gastroenterol Hepatol 2022:6799414. DOI: 10.1155/2022/6799414

Yang Y-X, Ahammed G, Wu C, *et al.,*2015. Crosstalk among jasmonate, salicylate and ethylene signaling pathways in plant disease and immune responses. Curr Protein Pept Sci 16:450-461. DOI: 10.2174/1389203716666150330141638

Yassin NY, AbouZid SF, El-Kalaawy AM, *et al.,* 2021. Tackling of renal carcinogenesis in wistar rats by silybum marianum total extract, silymarin, and silibinin via modulation of oxidative stress, apoptosis, Nrf2, PPARγ, NF-κB, and PI3K/Akt signaling pathways. Oxid Med Cell Longev 2021(1): 7665169. DOI: 10.1155/2021/7665169

Zakaria Z, Othman ZA, Nna VU, *et al.,* 2023. The promising roles of medicinal plants and bioactive compounds on hepatic lipid metabolism in the treatment of non-alcoholic fatty liver disease in animal models: Molecular targets. Arch Physiol Biochem 129:1262-1278. DOI: 10.1080/13813455.2021.1939387

Zarenezhad E, Abdulabbas HT, Kareem AS, *et al.,* 2023. Protective role of flavonoids quercetin and silymarin in the viral-associated inflammatory bowel disease: An updated review. Arch Microbiol 205(6): 252. DOI: 10.1007/s00203-023-03590-0

Zhang C, Sui Y, Liu S, *et al.,* 2023. Antiviral activity of bioactive molecules of silymarin against COVID-19 via in silico studies. Pharmaceuticals 16(10): 1479. https://doi.org/10.3390/ph16101479